Article:
Pu, K., Yang, S., Sheng, R. et al. (5 more authors) (2025) Chuanxiong-Danggui herb pair alleviated cognitive deficits of APP/PS1 mice by promoting mitophagy. Journal of Ethnopharmacology, 350. 119988. ISSN 0378-8741

https://doi.org/10.1016/j.jep.2025.119988

Graphical Abstract

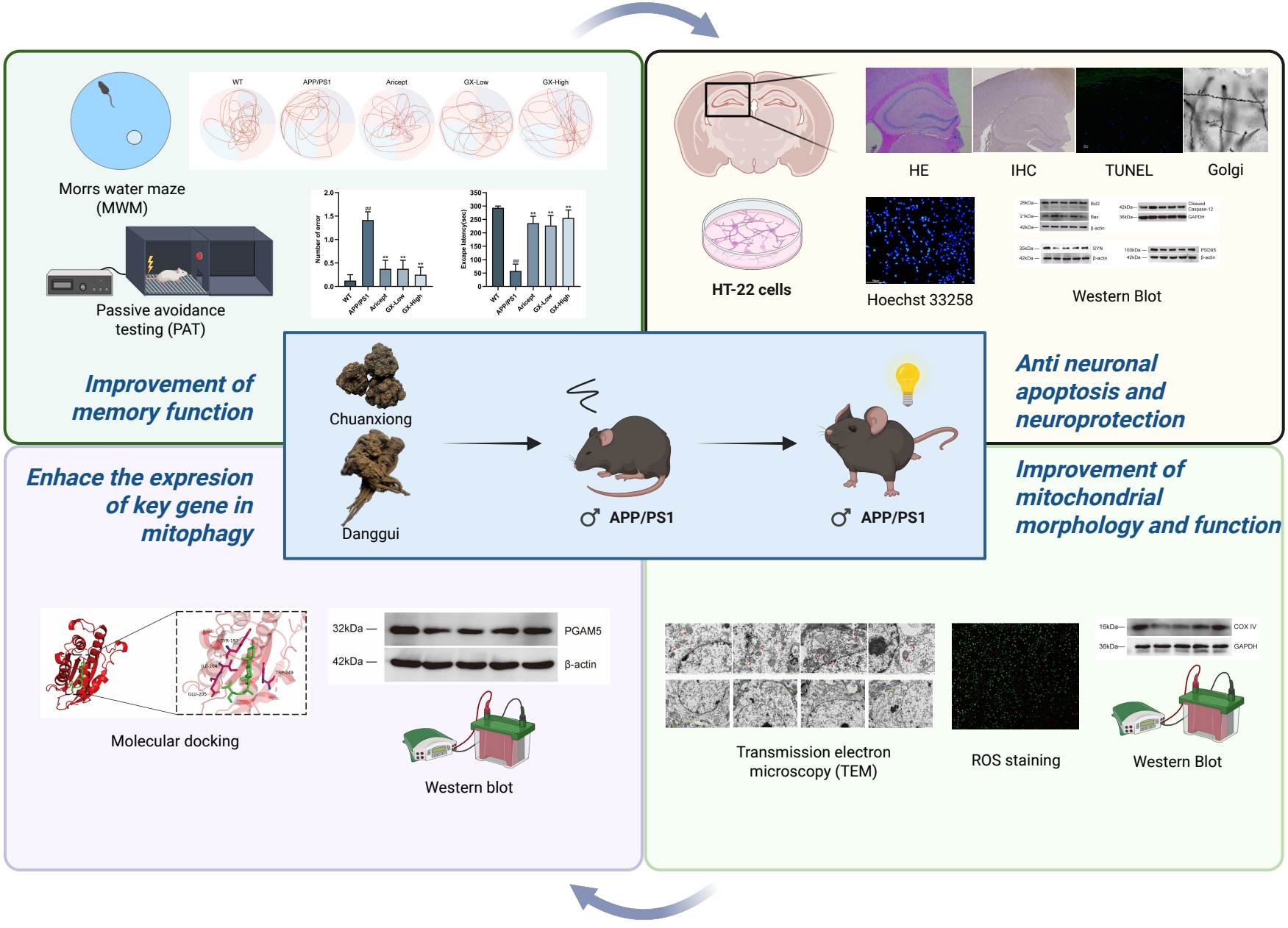

Chuanxiong-Danggui herb pair alleviated cognitive deficits of APP/PS1 mice by promoting mitophagy

Keting Pu [a,b,c 1], Simin Yang [a,b,c 1], Ruilin Sheng [a,b,c], Jie Chen [a,b,c], Yuan Dai[c,d], Ian C Wood[f*], Zhanqiong Zhong [e, f*], Shijun Xu [a,b,c *]

[a] State Key Laboratory of Southwestern Chinese Medicine Resources, Chengdu University of Traditional Chinese Medicine, 611137, P. R, China.

[b] School of Pharmacy, Chengdu University of Traditional Chinese Medicine, Chengdu, 611137, P. R, China.

[c] Institute of Material Medica Integration and Transformation for Brain Disorders, Chengdu University of Traditional Chinese Medicine, Chengdu, 611137, P. R, China.

[d] School of Health Preservation and Rehabilitation. Chengdu University of Traditional Chinese Medicine.Chengdu, 611137. China.

[e] School of Basic Medical Sciences, Chengdu University of Traditional Chinese Medicine, Chengdu, 611137, P. R, China.

[f] School of Biomedical Sciences, Faculty of Biological Sciences, University of Leeds, LS2 9JT, Leeds, UK.

[*]Correspondence author.

E-mail address: xushijun@cdutcm.edu.cn (S. Xu); zhongzhanqiong@cdutcm.edu.cn (Z. Zhong); i.c.wood@leeds.ac.uk (Ian C Wood).

[1]These authors equally contributed to this work.

ABSRTACT:

Ethnopharmacological relevance: Disruption of receptor-mediated mitophagy contributes to neuronal damage in Alzheimer's disease (AD). Chuanxiong-Danggui herb pair (CDHP) is classic herbal pair applied to treating neurodegenerative diseases including AD, Amyotrophic Lateral Sclerosis, Parkinson's disease. Though studies have demonstrated the neuroprotective effects of CDHP, the underlying mechanisms by which CDHP attenuates neuronal impairment of AD remains to be elucidated.

Aim of the study: The objective of this work was to investigate the anti-AD mechanism of CDHP in APP/PS1 mice.

Materials and methods: Behavioral assessments were conducted on C57BL/6J and APP/PS1 mice following CDHP treatment, alongside an evaluation of neuronal morphology in the hippocampal region. In vitro, HT-22 cells were induced by $A\beta_{25-35}$ before being treated with CDHP. The mechanisms of CDHP were investigated using

transmission electron microscopy, Golgi staining, immunofluorescence, siRNA, and Western blot analysis.

Results: Results from the passive avoidance test and the Morris water maze (MWM) indicated that CDHP significantly mitigated cognitive deficits of APP/PS1 mice, accompanied by a reduction of pathological damage in the CA1 and CA3 regions of hippocampus. Further testing found that a significant reduction in dendritic spines density was rescued by CDHP. Synaptophysin (SYN) and postsynaptic density protein 95 (PSD-95) were elevated in the CDHP group, while Aβ (β-amyloid) plaques deposition was significantly reduced. Simultaneously, CDHP markedly inhibited neuronal apoptosis through a decrease of the levels of Cleaved Caspase-12 and enhanced expression of Bcl-2/Bax, both in vivo and in vitro. Additionally, CDHP improved mitochondrial morphology and function in the AD model by decreasing abnormal mitochondria and increasing the expression of COXIV. Transmission electron microscopy (TEM) revealed that clear mitophagy-autophagosomes were nearly absent in APP/PS1 mice, while the expression of p62 and LC3B were elevated following CDHP treatment. Furthermore, CDHP increased the expression of the FUNDC1 and PGAM5 in APP/PS1 mice and AD-like cell models.

Conclusion: These findings suggest that CDHP mitigated cognitive dysfunction in APP/PS1 mice by enhancing mitophagy to reduce neuronal injury.

Keywords: Mitophagy, Alzheimer's disease, CDHP, FUNDC1,PGAM5

Highlight

1. Chuanxiong-Danggui herb pair (CDHP) alleviated cognitive deficits in an AD animal model.
2. CDHP promoted mitophagy in vivo and in vitro.
3. CDHP enhanced the expression of FUNDC1 and PGAM5 in vivo and vitro.

1. Introduction

Mitochondrial dysfunction is associated with various synaptic impairments, including axonal conduction, neurotransmitter release and reuptake, which may manifest in the early stages of AD (Skaper et al., 2017). Neuronal activity is

significantly reliant on functional mitochondria and the metabolic cost of normal neuronal function is high. Mitochondrial dysfunction exacerbates the pathological progression of AD and it is evident that mitochondrial deficits initiate neuronal damage, representing a critical pathological link in AD. Mitophagy serves as a vital mechanism for the clearance of damaged and dysfunctional mitochondria, thereby playing an essential role in maintaining mitochondrial functional homeostasis and neuronal synaptic plasticity (Mary et al., 2022). Research shows that mitochondrial dysfunction contributes to neurodegeneration in AD patients, while mitophagy enhancement has been shown to mitigate tau hyperphosphorylation and alleviate memory deficits in animal models (Fang et al., 2019).

Disruption of mitophagy is a significant mechanism leading to neuronal damage. Mitophagy, a form of selective autophagy, removes damaged or excess mitochondria and is facilitated mainly by the autophagosome-lysosome system (Y. Zhou et al., 2024). The process is crucial for mitochondrial quality control and mitigates damage by reactive oxygen species, which results in progressive accumulation of mitochondrial DNA (mtDNA) mutations and ultimately cell death. Impaired mitophagy has been associated with AD, potentially exacerbating the Aβ and tau pathologies through mechanisms involving in oxidative stress, chronic neuroinflammation and microglial activation (Song et al., 2021). A small-molecule that induces mitophagy has demonstrated therapeutic efficacy in both cellular and mouse models of AD (Um et al., 2024). In addition, ligands for the mitochondrial translocator protein, TSPO, have been shown to enhance P62/SQSTM1 gene expression and attenuate mitophagy deficits in cellular models (Fairley et al., 2024). Consequently, mitigating mitochondrial dysfunction and promoting mitophagy may be beneficial in reducing cognitive impairments associated with AD. Therefore, the protection of neurons, by enhancing mitophagy, has emerged as a novel target in the development of therapeutic strategies for AD (Katayama et al., 2020).

Mitophagy primarily involves two pathways, the PTEN-induced kinase 1/Parkin (PINK1/Parkin) or receptor mediated mitophagy (Wang et al., 2023). Although PINK1/Parkin mediated mitophagy is recognized for its role in various diseases,

including cerebral ischemia-reperfusion injury (X. Li et al., 2024), endometrial cancer (Wei et al., 2024) and neurodegenerative diseases (Yi et al., 2024), the significance of receptor-mediated mitophagy in the process of mitophagy is gaining increasing attention . Key receptors involved in this process include FUNDC1, Bcl-2/adenovirus E1B 19 kDa interacting protein 3 (BNIP3), BNIP3-like protein (NIX), Bcl-2 like 13 protein (Bcl2l13), Autophagy/Beclin-1 regulator-1 (AMBRA 1) (Schmid et al., 2022), FK506-binding protein 8 (FKBP8), Sorting and assembly machinery component 50 (SAMM50) and mitochondrial ferritin (FTMT) (Lee et al., 2018; Poole and Macleod, 2021). FUNDC1 is a critical receptor in the receptor-mitophagy pathway, directly binding to and recruiting LC3, thereby promoting mitophagy through the coordination of mitochondrial fission or fusion processes (Chen et al., 2016). Numerous studies have reported that FUNDC1-mediated protective mitophagy participates in the recovery process of various diseases, including heart failure, cardiovascular diseases, kidney disease and cerebral ischemia reperfusion injury (K. Li et al., 2024; Tian et al., 2022), indicating its significant role in addressing supply disorders (Li et al., 2021). Overexpression FUNDC1 has been shown to markedly enhance locomotor activity in amyotrophic lateral sclerosis (ALS) transgenic mice，suggesting a novel strategy for targeting FUNDC1-mediated mitophagy to improve outcomes for patients with ALS (X. Guo et al., 2024). Research on cerebral ischemia-reperfusion injury has indicated that tissue-type plasminogen activator exerts neuroprotective effects by increasing FUNDC1 expression, thereby inhibiting apoptosis and enhancing mitochondrial function (Y et al., 2021). Given the involvement of mitophagy in the pathogenesis of AD, FUNDC1 may play a pivotal role in mitophagy dysfunction.

Traditional Chinese medicine has been recognized for its therapeutic potential in treating neurodegenerative disorders. For instance, andrographolide has been shown to ameliorate cognitive impairment in an Apoe4 mouse model by initiating mitophagy and suppressing excessive neuroinflammation (Y. Zhou et al., 2024). Ginsenoside Rg1 may reduce β-amyloid (Aβ) deposits, restore mitophagy and ameliorate memory deficits in both cellular and animal models of AD via the classic PINK1-Parkin mitophagy pathway (N et al., 2023; She et al., 2024). Chuanxiong, Danggui, is derived from the

root of *Ligusticum sinense 'Chuanxiong' or Angelica sinensis (Oliv.)* Diels. Chuanxiong-Danggui herb pair (CDHP) is frequently used in traditional Chinese medicinal formulations for treatment of conditions such as heart failure, stroke, cerebral ischemia reperfusion injury, AD and Parkinson's disease (PD) (Chen et al., 2018). The active ingredients of CDHP include ligustilide, senkyunolide, angelica sinensis polysaccharide, tetramethylpyrazine, 3-butylphthalide, ferulic acid, coumarin, and flavonoids. Numerous studies have highlighted the neuroprotective roles of these active ingredients in neurodegenerative diseases. Angelica sinensis polysaccharides exhibits neuroprotective effects by inhibiting LPS-induced inflammatory injury in HT-22 cells (Zhou et al., 2019), and ameliorates memory dysfunction in AD rat models by activating BDNF/TrkB/CREB pathway (Du et al., 2020). Ligustilide has been shown to mitigate neuronal injury and exert neuroprotective effects following cerebral ischemia-reperfusion injury through promoting PINK1/Parkin-mediated mitophagy (Mao et al., 2022). Tetramethylpyrazine has been reported to attenuate neuroinflammatory responses in both LPS-induced cellular models and animal models, potentially through the activation of SIRT1 and suppression of NF-kB pathway (Chen et al., 2023). Notably, some active ingredients of CDHP significantly influence mitochondrial metabolism. For example, Ferulic acid has protective effects against ferroptosis by inhibiting the activity of mitochondrial complex I and reducing mitochondrial respiration (Günther et al., 2023). Therefore, we proposed a scientific hypothesis that CDHP exerts a neuroprotective role and reduction cognitive deficit in AD by promoting FUNDC1-mediated mitophagy.

This work aims to investigate the therapeutic potential of CDHP in promoting mitophagy and alleviation of cognitive decline in AD, furthermore, to testify the CDHP play the neuroprotection mediated the PGAM5/FUNDC1 or not. APP/PS1 mice were employed to evaluate the effects of CDHP on cognitive function through behavioral assessments and morphological analyses. The underlying molecular mechanisms of CDHP were further elucidated using HT-22 cells in an AD-like model.

2. Materials and methods

2.1 Reagents, antibodies and drugs

$A\beta_{25-35}$ peptide was procured from Chinese Peptide Company (AMTD51). Preparation of $A\beta_{25-35}$ peptide: 1 mg $A\beta_{25-35}$ was mixed with 943 uL hexafluoroisopropanol with $A\beta_{25-35}$ at room temperature for one hour. The peptide was dried by evaporation in 150 μL/unit aliquots. Froresuspensio, DMSO (15 μL) was added to each tube, followed by sonication in an ice bath for 10 mins. After addition of 1470 μL of cold PBS the sample was mixed thoroughly and incubated at 4 ℃ for seven days to obtain $A\beta_{25-35}$ oligomers. FUNDC1 antibody was purchased from ImmunoWay Biotechnology (YT5658, rabbit). β-actin (GB11001-100, rabbit), GAPDH (GB11002-100, rabbit), Goat Anti-Rabbit IgG (GB23303) and Goat Anti-Mouse IgG (GB23301) antibodies sourced from Servicebio. COX IV (00081701, rabbit) antibody sourced from MultiSciences, BAX (50599-2-Ig, rabbit) antibody and phosphoglycerate mutase family member 5 (PGAM5) (68116-1-Ig, mouse) were acquired from Proteintech, LC3 B (83506, mouse), Aβ (15126, mouse) and SQSTM1/p62 (5114S, rabbit) antibodies were obtained from Cell Signaling Technology. Bcl-2 (ab182858, rabbit), Synaptophysin (ab32127, rabbit) and Postsynaptic density protein 95 (PSD-95, ab13552, mouse) were purchased from Abcam. Aricept (2008002) acquired from Eisai (China) Pharmaceutical Company Limited. Angelica (220114-11) sourced from Chengdu Jiankang Pharmaceutical CO., Ltd, and Chuanxiong (2204104) purchased from Sichuan New Lotus Chinese Medical Drinks Co., Ltd.

The herbal formulation of CDHP consists of two Chinese herbs, *Chuanxiong Rhizoma* and *Radix Angelica sinensis*, in a ratio of 1:1. Equal weights of both herbs were combined with 10 times their weight in water, soaked for 30 mins, and then subjected to reflux heating extraction using a volatile oil extractor. The mixture was boiled and subsequently maintained at a gentle boil for 2 h, with two reflux extraction cycles performed. Following each cycle, the volatile oil was collected, cooled, filtered, and the combined filtrate was concentrated via vacuum spinning and freeze-drying to yield a lyophilized powder.

2.2 High Performance Liquid Chromatography (HPLC)

The quality of CDHP was assessed using HPLC. Reference substances, including Chlorogenic Acid (AZ22011851, Alfa Biotechnology, CHN), Ligustrazine

(AF8072604, Alfa Biotechnology, CHN), Caffeic Acid (AF21020856, Alfa Biotechnology, CHN) and Ferulic Acid (AF712632, Alfa Biotechnology, CHN) were accurately weighed, sonicated in methanol to prepare solutions at a concentration of 4 mg/mL. Reference substrates (250 μL of each) were combined to create a mixed standard solution at 1 mg/mL, and used to prepare mixed standards at concentrations of 0.1 mg/mL, 0.01 mg/mL, and 0.001 mg/mL. The lyophilized CDHP powder was dissolved in 20% methanol to achieve a concentration of 50 mg/mL. HPLC analysis was performed using a C18 column (Ultimate AQ-C18, Welch Materials, CHN) with a mobile phase consisting of methanol (A) and 0.2% acetic acid aqueous solution (B). The detection wavelength was set at 290 nm, with an injection volume of 10 μL, a column temperature of 25℃, and a flow rate of 0.8 mL/min.

2.3 Animals and Treatment

All animal experiments were conducted with approval from the Animal Ethics Committee of the Institute of Material Medica Integration and Transformation for Brain Diseases at Chengdu University of Traditional Chinese Medicine (No. IBD2202006). The animals were maintained at 23±1°C temperature, 50±5% humidity and 12-hour light-dark cycle. Male C57BL/6J (n=10) and APP/PS1 (n=50, 11~12 mice of each group) mice, were purchased from SPF (Beijing) Biotechnology Co. LTD, and were aged three months (License No.: 110324220105681135 and License No.: 110324220104497853). All animals were passed through an accommodation period, and APP/PS1 mice were randomly assigned to four groups: APP/PS1 group, Aricept group (0.92 mg/kg-d^{-1}) (Cao et al., 2017), CDHP-Low group (1.5 g/kg-d^{-1}), and CDHP-High group (3 g/kg-d^{-1}). CDHP lyophilized powder and Aricept were dissolved in purified water prior to administration. Dosages calculated based on the equivalent dose for mice and human as per the Chinese Pharmacopoeia. C57 BL/6J mice served as the wild-type (WT) group, which received pure water. All treatments, including drug administration and pure water, were conducted continuously for three months.

2.4 Cell Culture

HT-22 cells purchased from iCell Bioscience Inc (Shanghai, China). The cells were maintained in a high-glucose complete medium supplemented with 10% fetal bovine

serum, 1% Penicillin-Streptomycin. Cells were cultured at 37°C in a 5% CO_2 incubator. Cell viability was assessed by CCK-8 assay. Cells were seeded into 96-well plates at a density of 10,000 cells/well and set the groups as control, $A\beta_{25-35}$, $A\beta_{25-35}$+2.5 μg/mL CDHP, $A\beta_{25-35}$+5 μg/mL CDHP, and $A\beta_{25-35}$+10 μg/mL CDHP. Cells were treated with 25 μM $A\beta_{25-35}$ for 24 h, in the absence or presence of CDHP. After incubation, medium was removed, and replaced with 100μL of DMEM containing 10μL CCK-8 (BG0025, BIOGROUND, CHN). After 1 h at 37°C, the absorbance at 450 nm was measured using a microplate reader.

2.5 Behavioral Tests

2.5.1. Passive avoidance test（PAT）

The ability of mice to recall unpleasant experiences evaluated using the PAT system (TechMan Soft, CHN). The apparatus consisted of two compartments, one illuminated and the other dark and electrified. On the first day, mice were allowed to explore both compartments for 4 mins, with the dark compartment remaining unpowered. Following this acclimatization, the baffles were closed, and the dark compartment was electrified. Animals were then placed in the bright compartment, and the time taken for the mice to enter the dark compartment (escape latency) and the total number of shocks received (number of errors) recorded, with a maximum escape latency of 300 seconds. The procedure was repeated on the second day(Liu et al., 2014).

2.5.2. Morris Water Maze (MWM)

MWM apparatus (NOLDUS, Netherlands) were used to measure the spatial memory capacity of mice. During the training phase, a platform was positioned in the center of the third quadrant. Mice was placed in the maze and the time taken to find the platform recorded. If a mouse failed to find the platform within 2 mins, they were guided to the hidden platform and left there for three seconds. In the spatial exploration phase, the platform was removed, and the time and swimming path taken by mice and the duration of time within the target quadrant over a 120-second period was recorded(Costa-Mattioli et al., 2005).

2.6 Histopathological Analysis

Post-experiment, the brain of mice extracted and fixed with 4% paraformaldehyde

for one week, embedded and sectioned into 4-μm slices. After dewaxing, sections were stained with hematoxylin, eosin and Nissl. In brief, the sections underwent gradient dehydration using ethanol following dewaxing in xylene, were washed with water, and immersed in the hematoxylin and eosin or Nissl staining solutions. Finally, all sections sealed with neutral gum and visualized by microscope.

2.7 Immunohistochemistry (IHC)

Paraffin sections were dewaxed and hydrated, and 1 × Sodium citrate solution was used to repair the antigen at 100℃ for 20 mins. After cooling to room temperature and washing with PBS, the sections were treated with 3% H_2O_2 at room temperature for 5 mins. After washing, Aβ (1:800) was added dropwise and incubated at room temperature for 1 h. After washing by PBS, the secondary antibody in the immunohistochemistry kit (SV0004, Wuhan Boster) used for incubation and color with DAB solution. After washing with PBS, the nucleus was stained with hematoxylin. Finally, all sections were sealed with neutral gum and visualized by microscope.

2.8 Golgi staining

Fresh brain tissues excised and washed multiple times with purified water, and then stored in potassium dichromate solution and Mercury dichloride solution at room temperature. The solution replaced with fresh solution and maintained for two weeks. The tissue transferred to potassium chromate solution and exposed to light for a minimum of 72 hours. Sections were cut into 100-μm slices using a vibrating slicer, and stained according to the super Golgi kit (PK401, FD Neuro Technologies, INC, USA).

2.9 TUNEL Staining

Neuronal apoptosis was detected using a TUNEL kit (C1088, Beyotime Biotechnology, CHN) on paraffin-embedded mouse brain sections. Sections were incubated with 20 μg/mL DNase-free proteinase K at 37℃ for 20 mins. Following three washes with PBS, the preconfigured TUNEL solution was added dropwise and incubated at 37℃ for one hour. After three additional washes with PBS, sections were treated with an autofluorescence quencher containing DAPI (S2110, Solarbio, CHN),

and photographed using a fluorescence microscope.

2.10 Western Blot

Brain tissues of mice or HT-22 cells were homogenized in cold RIPA lysate buffer (CR2407036, Servicebio, CHN) containing phosphatase and protease inhibitors, and centrifuged (12,000 rpm/min) for 10 mins at 4°C. The concentration of total protein was quantified using BCA kit (BL521A, Biosharp, CHN). Proteins were denatured and subjected to electrophoresis on a 12% SDS-PAGE gel and transferred to polyvinylidene difluoride (PVDF) membranes. Membranes were blocked with 5% skimmed milk for one hour at room temperature, followed by overnight incubation with primary antibodies diluted in TBST with milk: FUNDC1 (1:800), β-actin (1:1000), COX IV (1:1000), SYN (1:200,000), PSD-95 (1:1000), SQSTM1/p62 (1:1000) PGAM5 (1:10000) and LC3 B (1:1000) were diluted by TBS. After washing with TBST three times, the PVDF membranes were incubated with the appropriate secondary antibody (1:1000) for one hour at room temperature. Membranes were imaged using the e-Blot system and images analyzed with Image-J.

2.11 Transmission electron microscopy (TEM)

Hippocampal regions of mice, approximately 1 mm^3 in size, were isolated on ice cleaned with saline, and put into electron microscope fixative. The tissue was fixed at room temperature for two hours using 1% osmium tetroxide. Following rinsing, gradient dehydration was performed, and then tissue was infiltrated and embedded at 60℃ using an acetone-812 embedding agent. Uranium-lead double staining performed after obtaining 60-80 nm sections, which dried overnight. Images were obtained using transmission electron microscopy.

2.12 Immunofluorescence of LC3B/TOM20 co-staining and reactive oxygen species (ROS)

HT-22 cells were co-stained with mouse anti-LC3B (1:200, #83506, CST, Cell Signaling Technology, USA) and rabbit anti-TOM20 (1:400, #GB111481, Servicebio, CHN) antibodies to observe co-localization. Cells were blocked for 30 mins at room temperature with 5% BSA solution, followed by overnight incubation with primary

antibodies at 4℃. Subsequently, cy3 goat anti-mouse (1:200, #GB21301, Servicebio, CHN) and 488 Goat anti-rabbit (1:200, #GB25303, Servicebio, CHN) were added and incubated for 2 h at room temperature. After washing, the samples treated with DAPI stain (#C0065, Solarbio, CHN) for 10 mins at room temperature. Following sealing, the fluorescence intensity of LC3B (red) and TOM20 (green) observed by a fluorescence microscope.

Reactive oxygen species were quantified using a detection kit (CA1410, Solarbio, CHN), DCFH-DA was diluted with serum-free medium at 1:10000 to a final concentration of 1 μmol/L in advance. After the cells were treated in 24-well plates, the culture medium was removed, and 200 μL/well diluted DCFH-DA was added and incubated in at 37 ℃ for 10 mins. The cells were gently washed three times with a serum-free medium to remove fully the DCFH-DA that did not enter the cells. Finally, observed by a fluorescence microscope.

2.13 Molecular docking

Based on the criteria of oral bioavailability (OB) 30% and drug-likeness (DL) 0.18 (Gao et al., 2024), the bioactive constituents of CDHP were identified using Traditional Chinese Medicine Systems Pharmacology Database and Analysis Platform (TCMSP, https://www.tcmsp-e.com/tcmspsearch.php). The 2D structure data of these compounds were obtained in sdf format from PubChem database (https://pubchem.ncbi.nlm.nih.gov/) and subsequently converted to mol2 format using Open Babel software (version 3.1.1). The 3D crystal structure of the target protein was obtained from Protein Data Bank database (PDB, https://www.rcsb.org/) and the protein structure was processed using PyMol software (version 3.0.3) to remove excess ligands (e.g., water molecules, Mg^{2+}, Cu^{2+}). The format of molecules and the protein were converted to pdpqt format using AutoDockTools software (version 1.5.6). Molecular docking was performed using Autodock software. The 3D docking results were visualized by PyMol.

2.14 Statistical analysis

Data shown are mean ± Standard Error of Mean (SEM) and were analyzed using *t-tests* or *Two-Way ANOVA,* as appropriate. Statistical significance was taken at $p < 0.05$

level.

3. Results

3.1 Analysis of active ingredients in CDHP using HPLC

Quality control assessment of the components in CDHP was conducted through HPLC. It was found that there were four peaks in the sample with the same retention time as the standards, confirming the presence of compounds that aligned with the mixed standards (chlorogenic acid, ligustrazine, caffeic acid, and ferulic acid). Notably, the ferulic acid content was quantified at 0.5824 mg/g (Figure 1) (Table 1), which complies with the standards set forth by the Chinese Pharmacopoeia (2020), thereby affirming the quality of CDHP.

Fig. 1 Analysis of active ingredients in CDHP. The four active ingredients constituents expected in CDHP: 1, Chlorogenic Acid, 2, Ligustrazine, 3, Caffeic Acid, and 4, Ferulic Acid, were evaluated using HPLC assays. The black, blue, yellow and green peaks represent mixed standards with varying concentration gradients, while the red peaks correspond to CDHP.

3.2 CDHP ameliorated cognitive impairment and pathologic morphology in APP/PS1 Mice

Behavioral assessments were performed to evaluate the impact of CDHP in APP/PS1 mice. In the passive avoidance experiment, APP/PS1 mice exhibited a significantly shorter escape latency and a higher number of errors compared to WT mice. However, following CDHP administration, the escape latency for APP/PS1 mice entering the dark box increased, and the number of errors decreased (Figure 2 A, B). In the MWM test, CDHP significantly enhanced the spatial memory capabilities of APP/PS1 mice, reducing the time taken to locate the platform and increasing the frequency of platform crossing, particularly in CDHP-H group (Figure 2 C-G). Additionally, histological evaluation via HE staining revealed the CA1 and CA3 regions of hippocampus in APP/PS1 mice atrophied compared to WT mice (Figure 2 H, I). Importantly, CDHP mitigated neuronal atrophy in this mouse model and ameliorated cognitive deficits.

Fig. 2 CDHP ameliorated cognitive impairment and brain pathology in APP/PS1 mice. A-B. Error counts and escape latency in the passive avoidance test (n=8). E. The escape latency of the training phase in the MWM test. （F (16, 178)=1.739, P=0.0432）. C, D, F. Frequency of platform crossing, total swimming distance and escape latency of the spatial exploration phase in the MWM test (n=8). G. Representative traces of each group in the MWM test. H. Representative images from HE analysis of the hippocampal CA1 and CA3 regions (n=5). Scale bars=100 μm. I. The width of CA1 and CA3 regions (n=5). Data are presented as mean ± SEM. $^{###}p<0.001$ compared with the WT group. $^{***}p<0.01$, $^{**}p<0.01$, $^{*}p<0.05$, compared with the APP/PS1 group.

3.3 CDHP increased dendritic spine density and reduced Aβ plaques in the brain of APP/PS1 Mice

Dendritic spines, which are protrusions on dendritic branches, serve as primary sites for synapse formation. Early synaptic dysfunction associated with tau pathology occurs in in dendritic spines in AD. The presence of stubby and mushroom-shaped dendritic spines are linked to memory function (Kasai et al., 2023). Golgi staining results showed that a significant reduction in spines density per 10 μm of dendrites in APP/PS1 mice, which were markedly ameliorated by CDHP treatment (Figure 3 A-C). Notably, the average percentage of stubby and mushroom-like dendritic spines in CDHP groups were higher than that of APP/PS1 mice (Figure 3 B). Furthermore, SYN and PSD-95 levels were markedly enhanced in the CDHP-H mice compared to APP/PS1 mice (Figure 3 D, E). Aβ plaques were detected in hippocampal and/or cortical region of all groups except WT mice, however, Aβ plaque deposition was significantly reduced in CDHP groups (Figure 3 F, G). These findings imply CDHP exerts neuroprotective effects by reducing Aβ plaque deposition in the brain of APP/PS1 mice.

Fig. 3 CDHP increased dendritic spine density and reduced Aβ plaques in the brain of APP/PS1 Mice. A. Example images of various dendritic spine types. B. Representative images of Golgi staining of dendritic spines across groups. Scale Bar=10 μm. C. Statistical analysis of dendritic spine density per 10 μm dendrites (n=3). D, E. Representative immunoblots and quantitative analyses of SYN and PSD-95 expression in mouse brain tissues (n=3). F. Representative images of the hippocampal region in each group and the area of Aβ plaques in cortical areas. Scale bar=100 or 200 μm. G. Percentage area of Aβ plaques of the brain in mouse brain (n=3). Data are presented as mean ± SEM. $^{###}p< 0.01$ compared with the WT group. $^{***}p<0.01$, $^{**}p<0.01$, $^{*}p<0.05$, compared with the APP/PS1 group.

3.4 CDHP inhibited neuronal apoptosis in vivo and in vitro

Neuronal cell death is a hallmark of neurodegenerative diseases, including PD and AD, with significant neuronal loss observed in key brain regions related to learning and memory (Chi et al., 2018). TUNEL staining was performed to assess neuronal apoptosis in the hippocampal region, and it showed a significantly higher number of apoptotic cells in APP/PS1 mice. The number of positive cells was lower in CDHP groups (Figure 4 A). Additionally, CDHP treatment significantly enhanced the expression of Bcl-2/Bax and decreased the levels of Cleaved Caspase-12 in the brain of APP/PS1 mice (Figure 4 B) and in HT-22 cells (Figure 4 C, D). These results suggest CDHP reduces neuronal apoptosis in APP/PS1 mice and $A\beta_{25-35}$-induced HT22 cells especially in high does group.

Fig. 4 CDHP inhibited neuronal apoptosis in vivo and in vitro. A. Representative images of TUNEL (green)/DAPI (blue) staining in the CA1 and CA3 regions of mouse mice (n=3). Scale bar=100 μm. Quantification of TUNEL-positive cells in each region. B. Representative immunoblots and quantitative analyses of Bcl-2, Bax, Cleaved Caspase-12, and GAPDH of mice brain (n=3). C. Representative immunoblots and quantitative analyses of Bcl-2, Bax, Cleaved Caspase-12, and GAPDH in HT-22 cells (n=3). D. Representative images with quantification of Hoechst 33258 staining in HT-22 cells (n=3). Scale bar=100 μm. Data are presented as mean ± SEM. $^{\#\#\#}p<0.001$, $^{\#\#}p<0.01$, compared with the WT or Control groups. $^{***}p<0.001$, $^{*}p<0.05$, compared to the APP/PS1 or $A\beta_{25-35}$ groups.

3.5 CDHP improved mitophagy through mitochondrial morphology and function in AD-like models

Abnormal neuronal apoptosis is often associated with mitochondria dysfunction. Mitochondria are essential for providing energy necessary for neuronal survival. Damaged mitochondria adversely affect neuronal structure and function, leading to energy deficits and the release of harmful substances that promote neuronal apoptosis. TEM images indicated that the morphology of mitochondria in the hippocampus of APP/PS1 mice was different to wild type mice, with blurred membrane boundaries and ridge, as well as damaged mitochondria with content leakage. However, the incidence of abnormal mitochondria significantly decreased following CDHP treatment (Figure 5

A). Additionally, in Aβ$_{25-35}$-induced HT-22 cells, CDHP-H markedly increased the levels of COXIV, a marker of mitochondrial function, (Figure 5 B). Levels of ROS in Aβ$_{25-35}$ treated cells were significantly decreased by CDHP in a dose dependent manner (Figure 5 C, D), suggesting that CDHP improves mitochondrial function in AD-like models.

The clearance of damaged mitochondria is primarily facilitated through mitophagy. TEM revealed that mitophagy-autophagosomes were nearly absent in the hippocampus of APP/PS1 mice compared to WT mice (Figure 6 A). CDHP treatment, prevented the reduction in mitophagy-autophagasomes. The expression levels of mitophagy substrate protein p62 was high and the autophagy marker protein LC3B was low in APP/PS1 mice compared to WT and Aβ$_{25-35}$-induced HT-22 cells compared to control but CDHP treatment restored levels to those seen in the WT animals (Figure 6 B) and non-induced HT-22 cells (Figure 6 C). All of the results shows that the CDHP treatment promote the mitophagy in AD.

Fig. 5 CDHP improved mitochondrial morphology and function in AD-like models. A. TEM results depicting mitochondrial morphology in the hippocampus (n=3). Scale bar =500 nm. B. Representative immunoblots and quantitative analyses of COX IV and GAPDH in Aβ$_{25-35}$-induced HT-22 cells (n=3). C-D. Immunofluorescence was used to detect the levels of ROS in HT-22 cells (n=3). Scale bar =100 μm. Data are presented as mean ± SEM. $^{###}p<0.001$ compared with the Control group. $^{*}p<0.05$, compared with the Aβ$_{25-35}$ group.

Fig. 6 CDHP improved mitophagy in vivo and in vitro. A. Representative TEM images of mitophagy in APP/PS1 mice (n=3). Scale bar=1 μm. B. Representative immunoblots and quantitative analyses of p62, LC3B and β-actin in mice (n=3). C. Representative immunoblots and quantitative analyses of p62, LC3B and β-actin in HT-22 cells. Data are presented as mean ± SEM. $^{###}p<0.001$, $^{##}p<0.01$ compared with the WT or Control groups. $^{***}p<0.001$, $^{**}p<0.01$, $^{*}p<0.05$, compared with the APP/PS1 or Aβ$_{25-35}$ groups.

3.6 CDHP enhanced PGAM5 and FUNDC1 in vivo and in vitro

To uncover the potential for CHDP to stimulate mitophagy, we used molecular docking of CHDP constituents with the mitochondrial phosphatase, Phosphoglycerate mutase family member 5 (PGAM5), a key driver of mitophagy. Eight bioactive constituents of CDHP were identified by TCMSP, the 2D structure data structure of them also list in Table 2, they are sitosterol, myricanone, mandenol, wallichilide,

senkyunone, perlolyrine, FA and stigmasterol. Subsequently, eight active ingredients were molecularly docked with PGAM5. Studies have shown that in molecular docking, when the affinity value is negative, it indicates that the molecule can bind to the protein. The smaller the value, the stronger the binding force between the two (Alsedfy et al., 2024). When the affinity is less than -7, it has a strong binding ability (Cui et al., 2020). Among the eight bioactive ingredients, except for mandenol, the affinity is ⩽-7 (Table 3) (Figure 7 A). The data indicates that the bioactive ingredients of CDHP could exert therapeutic effects by interacting with PGAM5.

To test the relationship between CDHP and PGAM5, the expression level of PGAM5 protein was measured. The brain tissue of APP/PS1 mice and HT-22 cells intervened by $A\beta_{25-35}$ was detected, and it was found that as predicted above, the protein level of PGAM5 in the AD model decreased significantly, and after the administration of CDHP, the expression level of PGAM5 increased significantly (Figure 7 B,C). This result suggests that CDHP may exhibit neuroprotection through increasing PGAM5.

Previous studies have indicated that the levels of mitophagy-related protein FUNDC1 diminished in AD cell models, and promoting FUNDC1-mediated mitophagy can protect neuronal function and mitigate stress-induced damage (Fang et al., 2019). Under normal conditions, the Ser13 and Tyr18 phosphorylation sites of FUNDC1 remain highly phosphorylated, inhibiting its interaction with LC3 and thereby preventing mitophagy. During mitochondrial depolarization and hypoxia, these phosphorylation sites are dephosphorylated, activating FUNDC1 and promoting its binding to LC3, which facilitates mitophagy (Cai et al., 2021; Yang et al., 2024). The FUNDC1 was mediated by Casein Kinase 2, Steroid receptor coactivator, ULK1 or PGAM5 (Liu et al., 2022). The expression level of FUNDC1 was increased significantly with the administration of CDHP (Figure S2).To sum up, we presumed the CDHP improve the expression of PGAM5, which is medicated the FUNDC1 to promote the mitophagy in AD.

Fig. 7 The bioactive ingredients in CDHP play a key role via PGAM5. A. Visualization results of molecular docking between bioactive ingredients in CDHP and PGAM5. B-C. Representative immunoblots and quantitative analyses of PGAM5 and β-actin in APP/PS1 mice brain and HT-22 cells (n=3). Data are presented as mean ± SEM.

$^{###}p<0.001$, compared with the WT or Control group. $^{***}p<0.001$, compared with the APP/PS1 or $A\beta_{25-35}$ group.

4 Discussion

Here we show that CDHP treatment significantly ameliorated cognitive impairment in the APP/PS1 model of AD. CDHP treatment appeared to reverse neuronal atrophy by enhancing the number of dendritic spines and reducing the presence of Aβ plaques in the brain. CDHP treatment was associated with an increase in the expression of mitochondrial proteins and a rise in the number of mitophagy bodies following CDHP administration. Mitophagy is a particular form of autophagy, that clears damaged or dysfunctional mitochondria, thereby contributing to cellular health and viability. This process is particularly vital in high energy-demanding cells, such as neurons, and is associated with various pathologies, including AD and Parkinson's disease. Furthermore, CDHP promoted the expression of PAGM5 and FUNDC1, 2 important proteins involved in mitophagy, suggesting a mechanism by which CDHP may promote mitophagy.

Angelica sinensis (Oliv.) Diels, a traditional Chinese medicinal herb, along with its root and extracts, has been shown to play a vital role in the treatment of various diseases, particularly those affecting the nervous system (Gao et al., 2023; Zeng et al., 2022). Similarly, the *Ligusticum sinense 'Chuanxiong'* exhibits comparable therapeutic properties. Evidence suggests that Ligustilide, the primary active compound derived from *Ligusticum chuanxiong hort* and *Angelica sinensis (Oliv.) Diels*, has neuroprotective effects in models of cerebral ischemia-reperfusion injury (Mao et al., 2022). Additionally, Polysaccharides, extracted different parts of *Angelica sinensis* root, have been reported to alleviate oxidative stress and exhibit anti-inflammatory and anti-oxidative properties in LPS-induced IPEC-J2 cells (Zou et al., 2022). Another study indicated that Angelica sinensis polysaccharide, when combined with Cisplatin, inhibited the expression of the key gene GPX4, promoting the ferroptosis and limiting the migration and invasion of ovarian cancer cells (W. Guo et al., 2024). Furthermore, Ligusticum chuanxiong Hort has been shown to facilitate the proliferation of neural stem cell, neurogenesis, and the preservation of mature neuron (Yu et al., 2021), as well

as to exert anti-neuroinflammation effects and stimulate the production of neural differentiation factor in rats following ischemia injury (Wang et al., 2020). Collectively, these findings support the protective effects of *Angelica sinensis (Oliv.) Diels* and Ligusticum sinense '*Chuanxiong*' across various disease contexts. In this study, we assert that CDHP exhibits neuroprotective activity in APP/PS1 mice and $A\beta_{25-35}$-induced HT-22 cells.

Our results demonstrate that CDHP ameliorates cognitive impairment and inhibits neuronal apoptosis in both APP/PS1 mice and HT-22 cells. Thus, we hypothesize a relationship between CDHP and mitochondrial function, which aligns with previous research findings. Mitophagy is a crucial mechanism for the removal of dysfunctional mitochondria and the maintenance of mitochondrial function, thereby ensuring intracellular homeostasis (Picca et al., 2023; Wang et al., 2023). Impaired mitophagy may exacerbate Aβ and tau pathologies through mechanisms involving oxidative stress, microglial activation, and chronic inflammation in AD (Song et al., 2021). Recent study has shown that long-term treatment with Urolithin A significantly enhances learning and memory functions in APP/PS1 mice by inducing mitophagy through the enhancement of cellular lysosomal functions (Hou et al., 2024). Similar findings have been reported for melatonin, which restored mitophagy by improving mitophagosome-lysosome fusion, reducing Aβ pathology, and enhancing cognition in transgenic mice (Chen et al., 2021). In our work, we posited a connection between CDHP and mitochondrial function. Subsequent transmission electron microscopy and Western Blot analyses revealed reduction in the number of abnormal mitochondria and elevation in the expression of mitochondrial function proteins following CDHP treatment in APP/PS1 mice and $A\beta_{25-35}$ induced HT-22 cells models. Interestingly, the number of mitophagy bodies increased in the hippocampus of APP/PS1 mice, while the levels of mitophagy substrate protein p62 decreased, and autophagy marker protein LC3B increased following CDHP treatment. Thus, we assert that CDHP enhances mitophagy in AD, and our data corroborate the notion that restored or improved mitophagy is beneficial for cognitive enhancement in this context. Unlike other pharmacological

agents or mechanisms, we propose that CDHP exerts its neuroprotective effects through mitophagy in AD. Traditional Chinese medicine has the characteristic of multi-target pharmacological effects. Therefore, our findings provide experimental evidence that CDHP treatment may alleviate cognitive dysfunction by improving mitophagy in AD.

Dendritic spines serve as the primary sites for synapse formation between neurons, their alterations are indicative of synaptic plasticity, which is essential for learning and long-term memory processes (Barrantes, 2024). Recent studies have demonstrated that in psychiatric patients elevated expression of NISCH lead to changed dendritic spine morphogenesis and impaired working memory (Yang et al., 2023). Additionally, early tau-related deficits have been linked to the accumulation of hyperphosphorylated tau within normal dendritic spines (Hoover et al., 2010). In our study, we observed a decrease in the number of functional dendritic spines in APP/PS1 mice, accompanied by an increase in Aβ plaques in the brain. Notably, the average percentage of stubby and mushroom-like dendritic spines in mice with CDHP was higher than that in APP/PS1 mice, and the levels of SYN and PSD-95 also increased in CDHP groups.

Mitophagy primarily involves two pathways, PINK1/Parkin-mediated pathway and the receptor-mediated pathway(Li et al., 2023). While PINK1/Parkin-mediated mitophagy pathway has been shown to play significant roles in neurodegenerative diseases in both murine models and Drosophila melanogaster with Parkin/PINK1 deficiencies, the body can compensate through a receptor-mediated mitophagy pathway that primarily involves mitochondrial membrane receptor proteins, such as FUNDC1, BNIP3 and NIX (D'Arcy, 2024). Shen-fu Injection activates the HIF- 1α/BNIP3 pathway to mediate mitophagy in ischemia-reperfusion injury(Chen et al., 2025), BNIP3-mediated mitophagy regulates the glycolytic shift and pro-inflammatory polarization in macrophages in obesity-related metabolic diseases(Kim et al., 2025), as well as NIX mediated mitophagy(X. Zhou et al., 2024). Thus, the receptor-mediated pathway is plays an essential role in diverse disease. FUNDC1 has been shown to preserve chondrocyte homeostasis by triggering mitophagy, with FUNDC1 knockdown or knockout leading to decreased mitophagy and exacerbated mitochondrial

dysfunction in osteoarthritis progression (Fang et al., 2023). Actived PGAM5 dephosphorylates FUNDC1 to initiate mitophagy. The reciprocal interaction of PGAM5 with FUNDC1 and BCL-xL, mediated by PGAM5 multimerization, work on mitophagy and apoptosis (Ma et al., 2020). Our dada shown that the CDHP treatment promoted mitophagy, and enhanced the expression of PGAM5 and FUNDC1.

5 Conclusion

In summary, CDHP has been shown to improve cognitive deficits and exert neuroprotective effects in APP/PS1 mice and $A\beta_{25-35}$-induced HT-22 cells. These effects correlate with a stimulated increase in mitophagy in vivo, and increased expression of PGAM5/FUNDC1. Our data highlight a potential mechanism for the neuroprotective effect of CDHP in AD and uncover a potential avenue for future therapeutic approaches.

Credit author statement

Keting Pu: Investigation, Methodology, Formal analysis, Validation, Visualization, Writing – original draft. **Simin Yang:** Investigation, Methodology, Validation. **Ruilin Sheng:** Methodology, Validation, Investigation. **Jie Chen:** Investigation. **Yuan Dai:** Supervision. **Ian C Wood:** Conceptualization, Supervision, revise & editing**. Zhanqiong Zhong:** Conceptualization, Funding acquisition, Investigation, Supervision, Methodology, Writing – original draft, Writing – review & editing. **Shijun Xu:** Design, Conceptualization, Data curation, Supervision, Writing – revise & editing, Funding acquisition. The authors agree to be responsible for all aspects of the manuscript ensuring the accuracy and integrity.

Declaration of competing interest

The authors declare that they have no known competing financial interests or personal relationships that could have appeared to influence the work reported in this paper.

Funding

This work was supported by National Natural Science Foundation of China (No. 82274240; No. 82074150,); Xinglin Scholars Project of Chengdu University of TCM (XJ2023001201; SYJS2024001).

Data availability

Data will be made available on request

Supplements

Fig. S1 A. Non-toxic concentration of CDHP on HT-22 cells (n=6). B. Concentrations of $A\beta_{25-35}$ intervention in the HT-22 cell model (n=6). C. Effects of different concentrations of CDHP on HT-22 cells with $A\beta_{25-35}$ intervention (n=6). Data are presented as mean ± SEM. $^{###}p<0.001$, $^{##}p<0.01$, $^{#}p<0.05$ compared with the Control group. $^{***}p<0.001$ compared with the $A\beta_{25-35}$ group.

Fig. S2 Representative immunoblots and quantitative analyses of FUNDC1, PGAM5 and β-actin (n=3). Data are presented as mean ± SEM. $^{###}p<0.001$ compared with the WT or Control groups. $^{**}p<0.01$, $^{*}p<0.05$, compared with the APP/PS1 or $A\beta_{25-35}$ groups.

Alsedfy, M.Y., Ebnalwaled, A.A., Moustafa, M., Said, A.H., 2024. Investigating the binding affinity, molecular dynamics, and ADMET properties of curcumin-IONPs as a mucoadhesive bioavailable oral treatment for iron deficiency anemia. Sci Rep 14, 22027. https://doi.org/10.1038/s41598-024-72577-8

Barrantes, F.J., 2024. Cognitive synaptopathy: synaptic and dendritic spine dysfunction in age-related cognitive disorders. Front Aging Neurosci 16, 1476909. https://doi.org/10.3389/fnagi.2024.1476909

Cai, Y., Yang, E., Yao, X., Zhang, X., Wang, Q., Wang, Y., Liu, J., Fan, W., Yi, K., Kang, C., Wu, J., 2021. FUNDC1-dependent mitophagy induced by tPA protects neurons against cerebral ischemia-reperfusion injury. Redox Biol 38, 101792. https://doi.org/10.1016/j.redox.2020.101792

Cao, J., Tang, Y., Li, Y., Gao, K., Shi, X., Li, Z., 2017. Behavioral Changes and Hippocampus Glucose Metabolism in APP/PS1 Transgenic Mice via Electro-acupuncture at Governor Vessel Acupoints. Front Aging Neurosci 9, 5. https://doi.org/10.3389/fnagi.2017.00005

Chen, C., Yang, C., Wang, J., Huang, X., Yu, H., Li, Shangming, Li, Shupeng, Zhang, Z., Liu, J., Yang, X., Liu, G.-P., 2021. Melatonin ameliorates cognitive deficits through improving mitophagy in a mouse model of Alzheimer's disease. J Pineal Res 71, e12774. https://doi.org/10.1111/jpi.12774

Chen, M., Chen, Z., Wang, Y., Tan, Z., Zhu, C., Li, Y., Han, Z., Chen, L., Gao, R., Liu, L., Chen, Q., 2016. Mitophagy receptor FUNDC1 regulates mitochondrial dynamics and mitophagy. Autophagy 12, 689–702. https://doi.org/10.1080/15548627.2016.1151580

Chen, Y., Peng, F., Yang, C., Hou, H., Xing, Z., Chen, J., Liu, L., Peng, C., Li, D., 2023. SIRT1 activation by 2,3,5,6-tetramethylpyrazine alleviates neuroinflammation via inhibiting M1 microglia polarization. Front Immunol 14, 1206513. https://doi.org/10.3389/fimmu.2023.1206513

Chen, Y., Wei, J., Zhang, Y., Sun, W., Li, Z., Wang, Q., Xu, X., Li, C., Li, P., 2018. Anti-endometriosis Mechanism of Jiawei Foshou San Based on Network Pharmacology. Front Pharmacol 9, 811. https://doi.org/10.3389/fphar.2018.00811

Chen, Z., Liu, T., Xiong, L., Liu, Z., 2025. Shen-fu Injection Modulates HIF- 1α/BNIP3-Mediated Mitophagy to Alleviate Myocardial Ischemia–Reperfusion Injury. Cardiovasc Toxicol. https://doi.org/10.1007/s12012-025-09993-3

Chi, H., Chang, H.-Y., Sang, T.-K., 2018. Neuronal Cell Death Mechanisms in Major Neurodegenerative Diseases. Int J Mol Sci 19, 3082. https://doi.org/10.3390/ijms19103082

Costa-Mattioli, M., Gobert, D., Harding, H., Herdy, B., Azzi, M., Bruno, M., Bidinosti, M., Mamou, C.B., Marcinkiewicz, E., Yoshida, M., Imataka, H., Claudio Cuello, A., Seidah, N., Sossin, W., Lacaille, J.-C., Ron, D., Nader, K., Sonenberg, N., 2005. Translational control of hippocampal synaptic plasticity and memory by the eIF2α kinase, GCN2. Nature 436, 1166–1173. https://doi.org/10.1038/nature03897

Cui, Q., Zhang, Y., Ma, Y., Yu, H., Zhao, X., Zhang, L., Ge, S., Zhang, G., Qin, X., 2020. A network pharmacology approach to investigate the mechanism of Shuxuening injection in the treatment of ischemic stroke. Journal of Ethnopharmacology 257, 112891. https://doi.org/10.1016/j.jep.2020.112891

D'Arcy, M.S., 2024. Mitophagy in health and disease. Molecular mechanisms, regulatory pathways, and therapeutic implications. Apoptosis. https://doi.org/10.1007/s10495-024-01977-y

Du, Q., Zhu, X., Si, J., 2020. Angelica polysaccharide ameliorates memory impairment in Alzheimer's disease rat through activating BDNF/TrkB/CREB pathway. Exp Biol Med (Maywood) 245, 1–10. https://doi.org/10.1177/1535370219894558

Fairley, L.H., Grimm, A., Herff, S.A., Eckert, A., 2024. Translocator protein (TSPO) ligands attenuate mitophagy deficits in the SH-SY5Y cellular model of Alzheimer's disease via the autophagy adaptor P62. Biochimie 224, 132–138. https://doi.org/10.1016/j.biochi.2024.01.012

Fang, E.F., Hou, Y., Palikaras, K., Adriaanse, B.A., Kerr, J.S., Yang, B., Lautrup, S., Hasan-Olive, M.M., Caponio, D., Dan, X., Rocktäschel, P., Croteau, D.L., Akbari, M., Greig, N.H., Fladby, T., Nilsen, H., Cader, M.Z., Mattson, M.P., Tavernarakis, N., Bohr, V.A., 2019. Mitophagy inhibits amyloid-β and tau pathology and reverses cognitive deficits in models of Alzheimer's disease. Nat Neurosci 22, 401–412. https://doi.org/10.1038/s41593-018-0332-9

Fang, G., Wen, X., Jiang, Z., Du, X., Liu, R., Zhang, C., Huang, G., Liao, W., Zhang, Z., 2023. FUNDC1/PFKP-mediated mitophagy induced by KD025 ameliorates cartilage degeneration in osteoarthritis. Mol Ther 31, 3594–3612. https://doi.org/10.1016/j.ymthe.2023.10.016

Gao, Y., Mo, S., Cao, H., Zhi, Y., Ma, X., Huang, Z., Li, B., Wu, J., Zhang, K., Jin, L., 2023. The efficacy and mechanism of Angelica sinensis (Oliv.) Diels root aqueous extract based on RNA sequencing and 16S rDNA sequencing in alleviating polycystic ovary syndrome. Phytomedicine 120, 155013. https://doi.org/10.1016/j.phymed.2023.155013

Gao, Y., Yang, Z., Ji, T., Zhou, P., Geng, L., Gao, X., 2024. Anti-papillary thyroid carcinoma effects of *dioscorea bulbifera* L. through ferroptosis and the PI3K/AKT pathway based on network pharmacology and experimental validation. Journal of Ethnopharmacology 326, 117912. https://doi.org/10.1016/j.jep.2024.117912

Günther, M., Dabare, S., Fuchs, J., Gunesch, S., Hofmann, J., Decker, M., Culmsee, C., 2023. Flavonoid-Phenolic Acid Hybrids Are Potent Inhibitors of Ferroptosis via Attenuation of Mitochondrial Impairment. Antioxidants (Basel) 13, 44. https://doi.org/10.3390/antiox13010044

Guo, W., Wang, W., Lei, F., Zheng, R., Zhao, X., Gu, Y., Yang, M., Tong, Y., Wang, Y., 2024. Angelica sinensis polysaccharide combined with cisplatin reverses cisplatin resistance of ovarian cancer by inducing ferroptosis via regulating GPX4. Biomed Pharmacother 175, 116680. https://doi.org/10.1016/j.biopha.2024.116680

Guo, X., Zhang, Z., Gu, J., Ke, P., Liu, J., Meng, Y., Zheng, W., Que, W., Fan, R., Luo, J., Xiao, F., 2024. FUDNC1-dependent mitophagy ameliorate motor neuron death in an amyotrophic lateral sclerosis mouse model. Neurobiol Dis 197, 106534. https://doi.org/10.1016/j.nbd.2024.106534

Hoover, B.R., Reed, M.N., Su, J., Penrod, R.D., Kotilinek, L.A., Grant, M.K., Pitstick, R., Carlson, G.A., Lanier, L.M., Yuan, L.-L., Ashe, K.H., Liao, D., 2010. Tau mislocalization to dendritic spines mediates synaptic dysfunction independently of neurodegeneration. Neuron 68, 1067–1081. https://doi.org/10.1016/j.neuron.2010.11.030

Hou, Y., Chu, X., Park, J.-H., Zhu, Q., Hussain, M., Li, Z., Madsen, H.B., Yang, B., Wei, Y., Wang, Y., Fang, E.F., Croteau, D.L., Bohr, V.A., 2024. Urolithin A improves Alzheimer's disease cognition and restores mitophagy and lysosomal functions. Alzheimers Dement 20, 4212–4233. https://doi.org/10.1002/alz.13847

Kasai, H., Ucar, H., Morimoto, Y., Eto, F., Okazaki, H., 2023. Mechanical transmission at spine synapses: Short-term potentiation and working memory. Curr Opin Neurobiol 80, 102706.

https://doi.org/10.1016/j.conb.2023.102706

Katayama, H., Hama, H., Nagasawa, K., Kurokawa, H., Sugiyama, M., Ando, R., Funata, M., Yoshida, N., Homma, M., Nishimura, T., Takahashi, M., Ishida, Y., Hioki, H., Tsujihata, Y., Miyawaki, A., 2020. Visualizing and Modulating Mitophagy for Therapeutic Studies of Neurodegeneration. Cell 181, 1176-1187.e16. https://doi.org/10.1016/j.cell.2020.04.025

Kim, S., Choi ,Cheoljun, Son ,Yeonho, Lee ,Junhyuck, Joo ,Sungug, and Lee, Y.-H., 2025. BNIP3-mediated mitophagy in macrophages regulates obesity-induced adipose tissue metaflammation. Autophagy 0, 1–19. https://doi.org/10.1080/15548627.2025.2487035

Lee, J.J., Sanchez-Martinez, A., Martinez Zarate, A., Benincá, C., Mayor, U., Clague, M.J., Whitworth, A.J., 2018. Basal mitophagy is widespread in Drosophila but minimally affected by loss of Pink1 or parkin. J Cell Biol 217, 1613–1622. https://doi.org/10.1083/jcb.201801044

Li, G., Li, J., Shao, R., Zhao, J., Chen, M., 2021. FUNDC1: A Promising Mitophagy Regulator at the Mitochondria-Associated Membrane for Cardiovascular Diseases. Front Cell Dev Biol 9, 788634. https://doi.org/10.3389/fcell.2021.788634

Li, J., Yang, D., Li, Z., Zhao, M., Wang, D., Sun, Z., Wen, P., Dai, Y., Gou, F., Ji, Y., Zhao, D., Yang, L., 2023. PINK1/Parkin-mediated mitophagy in neurodegenerative diseases. Ageing Research Reviews 84, 101817. https://doi.org/10.1016/j.arr.2022.101817

Li, K., Xia, X., Tong, Y., 2024. Multiple roles of mitochondrial autophagy receptor FUNDC1 in mitochondrial events and kidney disease. Front Cell Dev Biol 12, 1453365. https://doi.org/10.3389/fcell.2024.1453365

Li, X., Guan, L., Liu, Z., Du, Z., Yuan, Q., Zhou, F., Yang, X., Lv, M., Lv, L., 2024. Ubiquitination of ATAD3A by TRIM25 exacerbates cerebral ischemia-reperfusion injury via regulating PINK1/Parkin signaling pathway-mediated mitophagy. Free Radic Biol Med 224, 757–769. https://doi.org/10.1016/j.freeradbiomed.2024.09.029

Liu, H., Zang, C., Yuan, F., Ju, C., Shang, M., Ning, J., Yang, Y., Ma, J., Li, G., Bao, X., Zhang, D., 2022. The role of FUNDC1 in mitophagy, mitochondrial dynamics and human diseases. Biochemical Pharmacology 197, 114891. https://doi.org/10.1016/j.bcp.2021.114891

Liu, M., Chen, F., Sha, L., Wang, S., Tao, L., Yao, L., He, M., Yao, Z., Liu, H., Zhu, Z., Zhang, Z., Zheng, Z., Sha, X., Wei, M., 2014. (−)-Epigallocatechin-3-Gallate Ameliorates Learning and Memory Deficits by Adjusting the Balance of TrkA/p75NTR Signaling in APP/PS1 Transgenic Mice. Mol Neurobiol 49, 1350–1363. https://doi.org/10.1007/s12035-013-8608-2

Ma, K., Zhang, Z., Chang, R., Cheng, H., Mu, C., Zhao, T., Chen, L., Zhang, C., Luo, Q., Lin, J., Zhu, Y., Chen, Q., 2020. Dynamic PGAM5 multimers dephosphorylate BCL-xL or FUNDC1 to regulate mitochondrial and cellular fate. Cell Death Differ 27, 1036–1051. https://doi.org/10.1038/s41418-019-0396-4

Mao, Z., Tian, L., Liu, J., Wu, Q., Wang, N., Wang, G., Wang, Y., Seto, S., 2022. Ligustilide ameliorates hippocampal neuronal injury after cerebral ischemia reperfusion through activating PINK1/Parkin-dependent mitophagy. Phytomedicine 101, 154111. https://doi.org/10.1016/j.phymed.2022.154111

Mary, A., Eysert, F., Checler, F., Chami, M., 2022. Mitophagy in Alzheimer's disease: Molecular defects and therapeutic approaches. Molecular Psychiatry 28, 202. https://doi.org/10.1038/s41380-022-01631-6

N, W., J, Y., R, C., Y, L., S, L., Y, P., Q, L., Y, W., L, H., Y, S., Z, L., 2023. Ginsenoside Rg1 ameliorates Alzheimer's disease pathology via restoring mitophagy. Journal of ginseng research 47.

https://doi.org/10.1016/j.jgr.2022.12.001

Picca, A., Faitg, J., Auwerx, J., Ferrucci, L., D'Amico, D., 2023. Mitophagy in human health, ageing and disease. Nat Metab 5, 2047–2061. https://doi.org/10.1038/s42255-023-00930-8

Poole, L.P., Macleod, K.F., 2021. Mitophagy in tumorigenesis and metastasis. Cell Mol Life Sci 78, 3817–3851. https://doi.org/10.1007/s00018-021-03774-1

Schmid, E.T., Pyo, J.-H., Walker, D.W., 2022. Neuronal induction of BNIP3-mediated mitophagy slows systemic aging in Drosophila. Nat Aging 2, 494–507. https://doi.org/10.1038/s43587-022-00214-y

She, L., Sun, J., Xiong, L., Li, A., Li, L., Wu, H., Ren, J., Wang, W., Liang, G., Zhao, X., 2024. Ginsenoside RK1 improves cognitive impairments and pathological changes in Alzheimer's disease via stimulation of the AMPK/Nrf2 signaling pathway. Phytomedicine 122, 155168. https://doi.org/10.1016/j.phymed.2023.155168

Skaper, S.D., Facci, L., Zusso, M., Giusti, P., 2017. Synaptic Plasticity, Dementia and Alzheimer Disease. CNS Neurol Disord Drug Targets 16, 220–233. https://doi.org/10.2174/1871527316666170113120853

Song, M., Zhao, X., Song, F., 2021. Aging-Dependent Mitophagy Dysfunction in Alzheimer's Disease. Mol Neurobiol 58, 2362–2378. https://doi.org/10.1007/s12035-020-02248-y

Tian, W., Zhu, M., Zhou, Y., Mao, C., Zou, R., Cui, Y., Li, S., Zhu, J., Hu, C., 2022. Electroacupuncture Pretreatment Alleviates Cerebral Ischemia-Reperfusion Injury by Regulating Mitophagy via mTOR-ULK1/FUNDC1 Axis in Rats. J Stroke Cerebrovasc Dis 31, 106202. https://doi.org/10.1016/j.jstrokecerebrovasdis.2021.106202

Um, J.-H., Shin, D.J., Choi, S.M., Nathan, A.B.P., Kim, Y.Y., Lee, D.Y., Jeong, D.J., Kim, D.H., Kim, K.H., Kim, Y.H., Nah, J., Jeong, J.-H., Yoo, E., Shin, H.K., Park, H.T., Jo, J., Cho, J.H., Yun, J., 2024. Selective induction of Rab9-dependent alternative mitophagy using a synthetic derivative of isoquinoline alleviates mitochondrial dysfunction and cognitive deficits in Alzheimer's disease models. Theranostics 14, 56–74. https://doi.org/10.7150/thno.88718

Wang, M., Yao, M., Liu, J., Takagi, N., Yang, B., Zhang, M., Xu, L., Ren, J., Fan, X., Tian, F., 2020. Ligusticum chuanxiong exerts neuroprotection by promoting adult neurogenesis and inhibiting inflammation in the hippocampus of ME cerebral ischemia rats. J Ethnopharmacol 249, 112385. https://doi.org/10.1016/j.jep.2019.112385

Wang, S., Long, H., Hou, L., Feng, B., Ma, Z., Wu, Y., Zeng, Y., Cai, J., Zhang, D.-W., Zhao, G., 2023. The mitophagy pathway and its implications in human diseases. Signal Transduct Target Ther 8, 304. https://doi.org/10.1038/s41392-023-01503-7

Wei, X., Xiong, X., Wang, P., Zhang, S., Peng, D., 2024. SIRT1-mediated deacetylation of FOXO3 enhances mitophagy and drives hormone resistance in endometrial cancer. Mol Med 30, 147. https://doi.org/10.1186/s10020-024-00915-7

Y, C., E, Y., X, Y., X, Z., Q, W., Y, W., J, L., W, F., K, Y., C, K., J, W., 2021. FUNDC1-dependent mitophagy induced by tPA protects neurons against cerebral ischemia-reperfusion injury. Redox biology 38. https://doi.org/10.1016/j.redox.2020.101792

Yang, K., Yan, Y., Yu, A., Zhang, R., Zhang, Y., Qiu, Z., Li, Z., Zhang, Q., Wu, S., Li, F., 2024. Mitophagy in neurodegenerative disease pathogenesis. Neural Regen Res 19, 998–1005. https://doi.org/10.4103/1673-5374.385281

Yang, Z.-H., Cai, X., Ding, Z.-L., Li, W., Zhang, C.-Y., Huo, J.-H., Zhang, Y., Wang, L., Zhang, L.-M., Li, S.-W., Li, M., Zhang, C., Chang, H., Xiao, X., 2023. Identification of a psychiatric risk gene

NISCH at 3p21.1 GWAS locus mediating dendritic spine morphogenesis and cognitive function. BMC Med 21, 254. https://doi.org/10.1186/s12916-023-02931-6

Yi, J., Wang, H.-L., Lu, G., Zhang, H., Wang, Lina, Li, Z.-Y., Wang, Liming, Wu, Y., Xia, D., Fang, E.F., Shen, H.-M., 2024. Spautin-1 promotes PINK1-PRKN-dependent mitophagy and improves associative learning capability in an alzheimer disease animal model. Autophagy 1–22. https://doi.org/10.1080/15548627.2024.2383145

Yu, B., Yao, Y., Zhang, X., Ruan, M., Zhang, Z., Xu, L., Liang, T., Lu, J., 2021. Synergic Neuroprotection Between Ligusticum Chuanxiong Hort and Borneol Against Ischemic Stroke by Neurogenesis via Modulating Reactive Astrogliosis and Maintaining the Blood-Brain Barrier. Front Pharmacol 12, 666790. https://doi.org/10.3389/fphar.2021.666790

Zeng, P., Su, H.-F., Ye, C.-Y., Qiu, S.-W., Shi, A., Wang, J.-Z., Zhou, X.-W., Tian, Q., 2022. A Tau Pathogenesis-Based Network Pharmacology Approach for Exploring the Protections of Chuanxiong Rhizoma in Alzheimer's Disease. Front Pharmacol 13, 877806. https://doi.org/10.3389/fphar.2022.877806

Zhou, X., Lu, Q., Wang, Q., Chu, W., Huang, J., Yu, J., Nong, Y., Lu, W., 2024. Diltiazem Hydrochloride Protects Against Myocardial Ischemia/Reperfusion Injury in a BNIP3L/NIX-Mediated Mitophagy Manner. J Inflamm Res 17, 8905–8919. https://doi.org/10.2147/JIR.S493037

Zhou, Y., Guo, X., Chen, W., Liu, J., 2019. Angelica polysaccharide mitigates lipopolysaccharide-evoked inflammatory injury by regulating microRNA-10a in neuronal cell line HT22. Artif Cells Nanomed Biotechnol 47, 3194–3201. https://doi.org/10.1080/21691401.2019.1614595

Zhou, Y., Zhao, Q., Zhang, Y., Di, L., Xue, F., Xu, W., Gao, W., Guo, Y., He, Y., Kou, J., Qin, Y., Xie, X., Du, L., Han, G., Pang, X., 2024. A new andrographolide derivative ADA targeting SIRT3-FOXO3a signaling mitigates cognitive impairment by activating mitophagy and inhibiting neuroinflammation in Apoe4 mice. Phytomedicine 124, 155298. https://doi.org/10.1016/j.phymed.2023.155298

Zou, Y.-F., Li, C.-Y., Fu, Y.-P., Jiang, Q.-X., Peng, X., Li, L.-X., Song, X., Zhao, X.-H., Li, Y.-P., Chen, X.-F., Feng, B., Huang, C., Jia, R.-Y., Ye, G., Tang, H.-Q., Yin, Z.-Q., 2022. The comparison of preliminary structure and intestinal anti-inflammatory and anti-oxidative activities of polysaccharides from different root parts of Angelica sinensis (Oliv.) Diels. J Ethnopharmacol 295, 115446. https://doi.org/10.1016/j.jep.2022.115446

Chuanxiong-Danggui herb pair alleviated cognitive deficits of APP/PS1 mice by promoting mitophagy

Keting Pu [a,b,c 1], Simin Yang [a,b,c 1], Ruilin Sheng [a,b,c], Jie Chen [a,b,c], Yuan Dai[c,d], Ian C Wood[f*], Zhanqiong Zhong [e, f*], Shijun Xu [a,b,c *]

[a] State Key Laboratory of Southwestern Chinese Medicine Resources, Chengdu University of Traditional Chinese Medicine, 611137, P. R, China.

[b] School of Pharmacy, Chengdu University of Traditional Chinese Medicine, Chengdu, 611137, P. R, China.

[c] Institute of Material Medica Integration and Transformation for Brain Disorders, Chengdu University of Traditional Chinese Medicine, Chengdu, 611137, P. R, China.

[d] School of Health Preservation and Rehabilitation. Chengdu University of Traditional Chinese Medicine.Chengdu, 611137. China.

[e] School of Basic Medical Sciences, Chengdu University of Traditional Chinese Medicine, Chengdu, 611137, P. R, China.

[f] School of Biomedical Sciences, Faculty of Biological Sciences, University of Leeds, LS2 9JT, Leeds, UK.

[*]Correspondence author.

E-mail address: xushijun@cdutcm.edu.cn (S. Xu); zhongzhanqiong@cdutcm.edu.cn (Z. Zhong); i.c.wood@leeds.ac.uk (Ian C Wood).

[1]These authors equally contributed to this work.

ABSRTACT:

Ethnopharmacological relevance: Disruption of receptor-mediated mitophagy contributes to neuronal damage in Alzheimer's disease (AD). Chuanxiong-Danggui herb pair (CDHP) is classic herbal pair applied to treating neurodegenerative diseases including AD, Amyotrophic Lateral Sclerosis, Parkinson's disease. Though studies have demonstrated the neuroprotective effects of CDHP, the underlying mechanisms by which CDHP attenuates neuronal impairment of AD remains to be elucidated.

Aim of the study: The objective of this work was to investigate the anti-AD mechanism of CDHP in APP/PS1 mice.

Materials and methods: Behavioral assessments were conducted on C57BL/6J and APP/PS1 mice following CDHP treatment, alongside an evaluation of neuronal morphology in the hippocampal region. In vitro, HT-22 cells were induced by $A\beta_{25-35}$ before being treated with CDHP. The mechanisms of CDHP were investigated using

transmission electron microscopy, Golgi staining, immunofluorescence, siRNA, and Western blot analysis.

Results: Results from the passive avoidance test and the Morris water maze (MWM) indicated that CDHP significantly mitigated cognitive deficits of APP/PS1 mice, accompanied by a reduction of pathological damage in the CA1 and CA3 regions of hippocampus. Further testing found that a significant reduction in dendritic spines density was rescued by CDHP. Synaptophysin (SYN) and postsynaptic density protein 95 (PSD-95) were elevated in the CDHP group, while Aβ (β-amyloid) plaques deposition was significantly reduced. Simultaneously, CDHP markedly inhibited neuronal apoptosis through a decrease of the levels of Cleaved Caspase-12 and enhanced expression of Bcl-2/Bax, both in vivo and in vitro. Additionally, CDHP improved mitochondrial morphology and function in the AD model by decreasing abnormal mitochondria and increasing the expression of COXIV. Transmission electron microscopy (TEM) revealed that clear mitophagy-autophagosomes were nearly absent in APP/PS1 mice, while the expression of p62 and LC3B were elevated following CDHP treatment. Furthermore, CDHP increased the expression of the FUNDC1 and PGAM5 in APP/PS1 mice and AD-like cell models.

Conclusion: These findings suggest that CDHP mitigated cognitive dysfunction in APP/PS1 mice by enhancing mitophagy to reduce neuronal injury.

Keywords: Mitophagy, Alzheimer's disease, CDHP, FUNDC1,PGAM5

Highlight

1. Chuanxiong-Danggui herb pair (CDHP) alleviated cognitive deficits in an AD animal model.
2. CDHP promoted mitophagy in vivo and in vitro.
3. CDHP enhanced the expression of FUNDC1 and PGAM5 in vivo and vitro.

1. Introduction

Mitochondrial dysfunction is associated with various synaptic impairments, including axonal conduction, neurotransmitter release and reuptake, which may manifest in the early stages of AD (Skaper et al., 2017). Neuronal activity is

significantly reliant on functional mitochondria and the metabolic cost of normal neuronal function is high. Mitochondrial dysfunction exacerbates the pathological progression of AD and it is evident that mitochondrial deficits initiate neuronal damage, representing a critical pathological link in AD. Mitophagy serves as a vital mechanism for the clearance of damaged and dysfunctional mitochondria, thereby playing an essential role in maintaining mitochondrial functional homeostasis and neuronal synaptic plasticity (Mary et al., 2022). Research shows that mitochondrial dysfunction contributes to neurodegeneration in AD patients, while mitophagy enhancement has been shown to mitigate tau hyperphosphorylation and alleviate memory deficits in animal models (Fang et al., 2019).

Disruption of mitophagy is a significant mechanism leading to neuronal damage. Mitophagy, a form of selective autophagy, removes damaged or excess mitochondria and is facilitated mainly by the autophagosome-lysosome system (Y. Zhou et al., 2024). The process is crucial for mitochondrial quality control and mitigates damage by reactive oxygen species, which results in progressive accumulation of mitochondrial DNA (mtDNA) mutations and ultimately cell death. Impaired mitophagy has been associated with AD, potentially exacerbating the Aβ and tau pathologies through mechanisms involving in oxidative stress, chronic neuroinflammation and microglial activation (Song et al., 2021). A small-molecule that induces mitophagy has demonstrated therapeutic efficacy in both cellular and mouse models of AD (Um et al., 2024). In addition, ligands for the mitochondrial translocator protein, TSPO, have been shown to enhance P62/SQSTM1 gene expression and attenuate mitophagy deficits in cellular models (Fairley et al., 2024). Consequently, mitigating mitochondrial dysfunction and promoting mitophagy may be beneficial in reducing cognitive impairments associated with AD. Therefore, the protection of neurons, by enhancing mitophagy, has emerged as a novel target in the development of therapeutic strategies for AD (Katayama et al., 2020).

Mitophagy primarily involves two pathways, the PTEN-induced kinase 1/Parkin (PINK1/Parkin) or receptor mediated mitophagy (Wang et al., 2023). Although PINK1/Parkin mediated mitophagy is recognized for its role in various diseases,

including cerebral ischemia-reperfusion injury (X. Li et al., 2024), endometrial cancer (Wei et al., 2024) and neurodegenerative diseases (Yi et al., 2024), the significance of receptor-mediated mitophagy in the process of mitophagy is gaining increasing attention . Key receptors involved in this process include FUNDC1, Bcl-2/adenovirus E1B 19 kDa interacting protein 3 (BNIP3), BNIP3-like protein (NIX), Bcl-2 like 13 protein (Bcl2l13), Autophagy/Beclin-1 regulator-1 (AMBRA 1) (Schmid et al., 2022), FK506-binding protein 8 (FKBP8), Sorting and assembly machinery component 50 (SAMM50) and mitochondrial ferritin (FTMT) (Lee et al., 2018; Poole and Macleod, 2021). FUNDC1 is a critical receptor in the receptor-mitophagy pathway, directly binding to and recruiting LC3, thereby promoting mitophagy through the coordination of mitochondrial fission or fusion processes (Chen et al., 2016). Numerous studies have reported that FUNDC1-mediated protective mitophagy participates in the recovery process of various diseases, including heart failure, cardiovascular diseases, kidney disease and cerebral ischemia reperfusion injury (K. Li et al., 2024; Tian et al., 2022), indicating its significant role in addressing supply disorders (Li et al., 2021). Overexpression FUNDC1 has been shown to markedly enhance locomotor activity in amyotrophic lateral sclerosis (ALS) transgenic mice，suggesting a novel strategy for targeting FUNDC1-mediated mitophagy to improve outcomes for patients with ALS (X. Guo et al., 2024). Research on cerebral ischemia-reperfusion injury has indicated that tissue-type plasminogen activator exerts neuroprotective effects by increasing FUNDC1 expression, thereby inhibiting apoptosis and enhancing mitochondrial function (Y et al., 2021). Given the involvement of mitophagy in the pathogenesis of AD, FUNDC1 may play a pivotal role in mitophagy dysfunction.

Traditional Chinese medicine has been recognized for its therapeutic potential in treating neurodegenerative disorders. For instance, andrographolide has been shown to ameliorate cognitive impairment in an Apoe4 mouse model by initiating mitophagy and suppressing excessive neuroinflammation (Y. Zhou et al., 2024). Ginsenoside Rg1 may reduce β-amyloid (Aβ) deposits, restore mitophagy and ameliorate memory deficits in both cellular and animal models of AD via the classic PINK1-Parkin mitophagy pathway (N et al., 2023; She et al., 2024). Chuanxiong, Danggui, is derived from the

root of *Ligusticum sinense 'Chuanxiong' or Angelica sinensis (Oliv.)* Diels. Chuanxiong-Danggui herb pair (CDHP) is frequently used in traditional Chinese medicinal formulations for treatment of conditions such as heart failure, stroke, cerebral ischemia reperfusion injury, AD and Parkinson's disease (PD) (Chen et al., 2018). The active ingredients of CDHP include ligustilide, senkyunolide, angelica sinensis polysaccharide, tetramethylpyrazine, 3-butylphthalide, ferulic acid, coumarin, and flavonoids. Numerous studies have highlighted the neuroprotective roles of these active ingredients in neurodegenerative diseases. Angelica sinensis polysaccharides exhibits neuroprotective effects by inhibiting LPS-induced inflammatory injury in HT-22 cells (Zhou et al., 2019), and ameliorates memory dysfunction in AD rat models by activating BDNF/TrkB/CREB pathway (Du et al., 2020). Ligustilide has been shown to mitigate neuronal injury and exert neuroprotective effects following cerebral ischemia-reperfusion injury through promoting PINK1/Parkin-mediated mitophagy (Mao et al., 2022). Tetramethylpyrazine has been reported to attenuate neuroinflammatory responses in both LPS-induced cellular models and animal models, potentially through the activation of SIRT1 and suppression of NF-kB pathway (Chen et al., 2023). Notably, some active ingredients of CDHP significantly influence mitochondrial metabolism. For example, Ferulic acid has protective effects against ferroptosis by inhibiting the activity of mitochondrial complex I and reducing mitochondrial respiration (Günther et al., 2023). Therefore, we proposed a scientific hypothesis that CDHP exerts a neuroprotective role and reduction cognitive deficit in AD by promoting FUNDC1-mediated mitophagy.

This work aims to investigate the therapeutic potential of CDHP in promoting mitophagy and alleviation of cognitive decline in AD, furthermore, to testify the CDHP play the neuroprotection mediated the PGAM5/FUNDC1 or not. APP/PS1 mice were employed to evaluate the effects of CDHP on cognitive function through behavioral assessments and morphological analyses. The underlying molecular mechanisms of CDHP were further elucidated using HT-22 cells in an AD-like model.

2. Materials and methods

2.1 Reagents, antibodies and drugs

$A\beta_{25-35}$ peptide was procured from Chinese Peptide Company (AMTD51). Preparation of $A\beta_{25-35}$ peptide: 1 mg $A\beta_{25-35}$ was mixed with 943 uL hexafluoroisopropanol with $A\beta_{25-35}$ at room temperature for one hour. The peptide was dried by evaporation in 150 μL/unit aliquots. Froresuspensio, DMSO (15 μL) was added to each tube, followed by sonication in an ice bath for 10 mins. After addition of 1470 μL of cold PBS the sample was mixed thoroughly and incubated at 4 ℃ for seven days to obtain $A\beta_{25-35}$ oligomers. FUNDC1 antibody was purchased from ImmunoWay Biotechnology (YT5658, rabbit). β-actin (GB11001-100, rabbit), GAPDH (GB11002-100, rabbit), Goat Anti-Rabbit IgG (GB23303) and Goat Anti-Mouse IgG (GB23301) antibodies sourced from Servicebio. COX IV (00081701, rabbit) antibody sourced from MultiSciences, BAX (50599-2-Ig, rabbit) antibody and phosphoglycerate mutase family member 5 (PGAM5) (68116-1-Ig, mouse) were acquired from Proteintech, LC3 B (83506, mouse), Aβ (15126, mouse) and SQSTM1/p62 (5114S, rabbit) antibodies were obtained from Cell Signaling Technology. Bcl-2 (ab182858, rabbit), Synaptophysin (ab32127, rabbit) and Postsynaptic density protein 95 (PSD-95, ab13552, mouse) were purchased from Abcam. Aricept (2008002) acquired from Eisai (China) Pharmaceutical Company Limited. Angelica (220114-11) sourced from Chengdu Jiankang Pharmaceutical CO., Ltd, and Chuanxiong (2204104) purchased from Sichuan New Lotus Chinese Medical Drinks Co., Ltd.

The herbal formulation of CDHP consists of two Chinese herbs, *Chuanxiong Rhizoma* and *Radix Angelica sinensis*, in a ratio of 1:1. Equal weights of both herbs were combined with 10 times their weight in water, soaked for 30 mins, and then subjected to reflux heating extraction using a volatile oil extractor. The mixture was boiled and subsequently maintained at a gentle boil for 2 h, with two reflux extraction cycles performed. Following each cycle, the volatile oil was collected, cooled, filtered, and the combined filtrate was concentrated via vacuum spinning and freeze-drying to yield a lyophilized powder.

2.2 High Performance Liquid Chromatography (HPLC)

The quality of CDHP was assessed using HPLC. Reference substances, including Chlorogenic Acid (AZ22011851, Alfa Biotechnology, CHN), Ligustrazine

(AF8072604, Alfa Biotechnology, CHN), Caffeic Acid (AF21020856, Alfa Biotechnology, CHN) and Ferulic Acid (AF712632, Alfa Biotechnology, CHN) were accurately weighed, sonicated in methanol to prepare solutions at a concentration of 4 mg/mL. Reference substrates (250 μL of each) were combined to create a mixed standard solution at 1 mg/mL, and used to prepare mixed standards at concentrations of 0.1 mg/mL, 0.01 mg/mL, and 0.001 mg/mL. The lyophilized CDHP powder was dissolved in 20% methanol to achieve a concentration of 50 mg/mL. HPLC analysis was performed using a C18 column (Ultimate AQ-C18, Welch Materials, CHN) with a mobile phase consisting of methanol (A) and 0.2% acetic acid aqueous solution (B). The detection wavelength was set at 290 nm, with an injection volume of 10 μL, a column temperature of 25℃, and a flow rate of 0.8 mL/min.

2.3 Animals and Treatment

All animal experiments were conducted with approval from the Animal Ethics Committee of the Institute of Material Medica Integration and Transformation for Brain Diseases at Chengdu University of Traditional Chinese Medicine (No. IBD2202006). The animals were maintained at 23±1°C temperature, 50±5% humidity and 12-hour light-dark cycle. Male C57BL/6J (n=10) and APP/PS1 (n=50, 11~12 mice of each group) mice, were purchased from SPF (Beijing) Biotechnology Co. LTD, and were aged three months (License No.: 110324220105681135 and License No.: 110324220104497853). All animals were passed through an accommodation period, and APP/PS1 mice were randomly assigned to four groups: APP/PS1 group, Aricept group (0.92 mg/kg-d^{-1}) (Cao et al., 2017), CDHP-Low group (1.5 g/kg-d^{-1}), and CDHP-High group (3 g/kg-d^{-1}). CDHP lyophilized powder and Aricept were dissolved in purified water prior to administration. Dosages calculated based on the equivalent dose for mice and human as per the Chinese Pharmacopoeia. C57 BL/6J mice served as the wild-type (WT) group, which received pure water. All treatments, including drug administration and pure water, were conducted continuously for three months.

2.4 Cell Culture

HT-22 cells purchased from iCell Bioscience Inc (Shanghai, China). The cells were maintained in a high-glucose complete medium supplemented with 10% fetal bovine

serum, 1% Penicillin-Streptomycin. Cells were cultured at 37°C in a 5% CO_2 incubator. Cell viability was assessed by CCK-8 assay. Cells were seeded into 96-well plates at a density of 10,000 cells/well and set the groups as control, $A\beta_{25-35}$, $A\beta_{25-35}$+2.5 μg/mL CDHP, $A\beta_{25-35}$+5 μg/mL CDHP, and $A\beta_{25-35}$+10 μg/mL CDHP. Cells were treated with 25 μM $A\beta_{25-35}$ for 24 h, in the absence or presence of CDHP. After incubation, medium was removed, and replaced with 100μL of DMEM containing 10μL CCK-8 (BG0025, BIOGROUND, CHN). After 1 h at 37°C, the absorbance at 450 nm was measured using a microplate reader.

2.5 Behavioral Tests

2.5.1. Passive avoidance test（PAT）

The ability of mice to recall unpleasant experiences evaluated using the PAT system (TechMan Soft, CHN). The apparatus consisted of two compartments, one illuminated and the other dark and electrified. On the first day, mice were allowed to explore both compartments for 4 mins, with the dark compartment remaining unpowered. Following this acclimatization, the baffles were closed, and the dark compartment was electrified. Animals were then placed in the bright compartment, and the time taken for the mice to enter the dark compartment (escape latency) and the total number of shocks received (number of errors) recorded, with a maximum escape latency of 300 seconds. The procedure was repeated on the second day(Liu et al., 2014).

2.5.2. Morris Water Maze (MWM)

MWM apparatus (NOLDUS, Netherlands) were used to measure the spatial memory capacity of mice. During the training phase, a platform was positioned in the center of the third quadrant. Mice was placed in the maze and the time taken to find the platform recorded. If a mouse failed to find the platform within 2 mins, they were guided to the hidden platform and left there for three seconds. In the spatial exploration phase, the platform was removed, and the time and swimming path taken by mice and the duration of time within the target quadrant over a 120-second period was recorded(Costa-Mattioli et al., 2005).

2.6 Histopathological Analysis

Post-experiment, the brain of mice extracted and fixed with 4% paraformaldehyde

for one week, embedded and sectioned into 4-μm slices. After dewaxing, sections were stained with hematoxylin, eosin and Nissl. In brief, the sections underwent gradient dehydration using ethanol following dewaxing in xylene, were washed with water, and immersed in the hematoxylin and eosin or Nissl staining solutions. Finally, all sections sealed with neutral gum and visualized by microscope.

2.7 Immunohistochemistry (IHC)

Paraffin sections were dewaxed and hydrated, and 1 × Sodium citrate solution was used to repair the antigen at 100℃ for 20 mins. After cooling to room temperature and washing with PBS, the sections were treated with 3% H_2O_2 at room temperature for 5 mins. After washing, Aβ (1:800) was added dropwise and incubated at room temperature for 1 h. After washing by PBS, the secondary antibody in the immunohistochemistry kit (SV0004, Wuhan Boster) used for incubation and color with DAB solution. After washing with PBS, the nucleus was stained with hematoxylin. Finally, all sections were sealed with neutral gum and visualized by microscope.

2.8 Golgi staining

Fresh brain tissues excised and washed multiple times with purified water, and then stored in potassium dichromate solution and Mercury dichloride solution at room temperature. The solution replaced with fresh solution and maintained for two weeks. The tissue transferred to potassium chromate solution and exposed to light for a minimum of 72 hours. Sections were cut into 100-μm slices using a vibrating slicer, and stained according to the super Golgi kit (PK401, FD Neuro Technologies, INC, USA).

2.9 TUNEL Staining

Neuronal apoptosis was detected using a TUNEL kit (C1088, Beyotime Biotechnology, CHN) on paraffin-embedded mouse brain sections. Sections were incubated with 20 μg/mL DNase-free proteinase K at 37℃ for 20 mins. Following three washes with PBS, the preconfigured TUNEL solution was added dropwise and incubated at 37℃ for one hour. After three additional washes with PBS, sections were treated with an autofluorescence quencher containing DAPI (S2110, Solarbio, CHN),

and photographed using a fluorescence microscope.

2.10 Western Blot

Brain tissues of mice or HT-22 cells were homogenized in cold RIPA lysate buffer (CR2407036, Servicebio, CHN) containing phosphatase and protease inhibitors, and centrifuged (12,000 rpm/min) for 10 mins at 4°C. The concentration of total protein was quantified using BCA kit (BL521A, Biosharp, CHN). Proteins were denatured and subjected to electrophoresis on a 12% SDS-PAGE gel and transferred to polyvinylidene difluoride (PVDF) membranes. Membranes were blocked with 5% skimmed milk for one hour at room temperature, followed by overnight incubation with primary antibodies diluted in TBST with milk: FUNDC1 (1:800), β-actin (1:1000), COX IV (1:1000), SYN (1:200,000), PSD-95 (1:1000), SQSTM1/p62 (1:1000) PGAM5 (1:10000) and LC3 B (1:1000) were diluted by TBS. After washing with TBST three times, the PVDF membranes were incubated with the appropriate secondary antibody (1:1000) for one hour at room temperature. Membranes were imaged using the e-Blot system and images analyzed with Image-J.

2.11 Transmission electron microscopy (TEM)

Hippocampal regions of mice, approximately 1 mm^3 in size, were isolated on ice cleaned with saline, and put into electron microscope fixative. The tissue was fixed at room temperature for two hours using 1% osmium tetroxide. Following rinsing, gradient dehydration was performed, and then tissue was infiltrated and embedded at 60℃ using an acetone-812 embedding agent. Uranium-lead double staining performed after obtaining 60-80 nm sections, which dried overnight. Images were obtained using transmission electron microscopy.

2.12 Immunofluorescence of LC3B/TOM20 co-staining and reactive oxygen species (ROS)

HT-22 cells were co-stained with mouse anti-LC3B (1:200, #83506, CST, Cell Signaling Technology, USA) and rabbit anti-TOM20 (1:400, #GB111481, Servicebio, CHN) antibodies to observe co-localization. Cells were blocked for 30 mins at room temperature with 5% BSA solution, followed by overnight incubation with primary

antibodies at 4℃. Subsequently, cy3 goat anti-mouse (1:200, #GB21301, Servicebio, CHN) and 488 Goat anti-rabbit (1:200, #GB25303, Servicebio, CHN) were added and incubated for 2 h at room temperature. After washing, the samples treated with DAPI stain (#C0065, Solarbio, CHN) for 10 mins at room temperature. Following sealing, the fluorescence intensity of LC3B (red) and TOM20 (green) observed by a fluorescence microscope.

Reactive oxygen species were quantified using a detection kit (CA1410, Solarbio, CHN), DCFH-DA was diluted with serum-free medium at 1:10000 to a final concentration of 1 μmol/L in advance. After the cells were treated in 24-well plates, the culture medium was removed, and 200 μL/well diluted DCFH-DA was added and incubated in at 37 ℃ for 10 mins. The cells were gently washed three times with a serum-free medium to remove fully the DCFH-DA that did not enter the cells. Finally, observed by a fluorescence microscope.

2.13 Molecular docking

Based on the criteria of oral bioavailability (OB) 30% and drug-likeness (DL) 0.18 (Gao et al., 2024), the bioactive constituents of CDHP were identified using Traditional Chinese Medicine Systems Pharmacology Database and Analysis Platform (TCMSP, https://www.tcmsp-e.com/tcmspsearch.php). The 2D structure data of these compounds were obtained in sdf format from PubChem database (https://pubchem.ncbi.nlm.nih.gov/) and subsequently converted to mol2 format using Open Babel software (version 3.1.1). The 3D crystal structure of the target protein was obtained from Protein Data Bank database (PDB, https://www.rcsb.org/) and the protein structure was processed using PyMol software (version 3.0.3) to remove excess ligands (e.g., water molecules, Mg^{2+}, Cu^{2+}). The format of molecules and the protein were converted to pdpqt format using AutoDockTools software (version 1.5.6). Molecular docking was performed using Autodock software. The 3D docking results were visualized by PyMol.

2.14 Statistical analysis

Data shown are mean ± Standard Error of Mean (SEM) and were analyzed using *t-tests* or *Two-Way ANOVA,* as appropriate. Statistical significance was taken at $p < 0.05$

level.

3. Results

3.1 Analysis of active ingredients in CDHP using HPLC

Quality control assessment of the components in CDHP was conducted through HPLC. It was found that there were four peaks in the sample with the same retention time as the standards, confirming the presence of compounds that aligned with the mixed standards (chlorogenic acid, ligustrazine, caffeic acid, and ferulic acid). Notably, the ferulic acid content was quantified at 0.5824 mg/g (Figure 1) (Table 1), which complies with the standards set forth by the Chinese Pharmacopoeia (2020), thereby affirming the quality of CDHP.

Fig. 1 Analysis of active ingredients in CDHP. The four active ingredients constituents expected in CDHP: 1, Chlorogenic Acid, 2, Ligustrazine, 3, Caffeic Acid, and 4, Ferulic Acid, were evaluated using HPLC assays. The black, blue, yellow and green peaks represent mixed standards with varying concentration gradients, while the red peaks correspond to CDHP.

3.2 CDHP ameliorated cognitive impairment and pathologic morphology in APP/PS1 Mice

Behavioral assessments were performed to evaluate the impact of CDHP in APP/PS1 mice. In the passive avoidance experiment, APP/PS1 mice exhibited a significantly shorter escape latency and a higher number of errors compared to WT mice. However, following CDHP administration, the escape latency for APP/PS1 mice entering the dark box increased, and the number of errors decreased (Figure 2 A, B). In the MWM test, CDHP significantly enhanced the spatial memory capabilities of APP/PS1 mice, reducing the time taken to locate the platform and increasing the frequency of platform crossing, particularly in CDHP-H group (Figure 2 C-G). Additionally, histological evaluation via HE staining revealed the CA1 and CA3 regions of hippocampus in APP/PS1 mice atrophied compared to WT mice (Figure 2 H, I). Importantly, CDHP mitigated neuronal atrophy in this mouse model and ameliorated cognitive deficits.

Fig. 2 CDHP ameliorated cognitive impairment and brain pathology in APP/PS1 mice. A-B. Error counts and escape latency in the passive avoidance test (n=8). E. The escape latency of the training phase in the MWM test.（F (16, 178)=1.739, P=0.0432）. C, D, F. Frequency of platform crossing, total swimming distance and escape latency of the spatial exploration phase in the MWM test (n=8). G. Representative traces of each group in the MWM test. H. Representative images from HE analysis of the hippocampal CA1 and CA3 regions (n=5). Scale bars=100 μm. I. The width of CA1 and CA3 regions (n=5). Data are presented as mean ± SEM. $^{###}p<0.001$ compared with the WT group. $^{***}p<0.01$, $^{**}p<0.01$, $^{*}p<0.05$, compared with the APP/PS1 group.

3.3 CDHP increased dendritic spine density and reduced Aβ plaques in the brain of APP/PS1 Mice

Dendritic spines, which are protrusions on dendritic branches, serve as primary sites for synapse formation. Early synaptic dysfunction associated with tau pathology occurs in in dendritic spines in AD. The presence of stubby and mushroom-shaped dendritic spines are linked to memory function (Kasai et al., 2023). Golgi staining results showed that a significant reduction in spines density per 10 μm of dendrites in APP/PS1 mice, which were markedly ameliorated by CDHP treatment (Figure 3 A-C). Notably, the average percentage of stubby and mushroom-like dendritic spines in CDHP groups were higher than that of APP/PS1 mice (Figure 3 B). Furthermore, SYN and PSD-95 levels were markedly enhanced in the CDHP-H mice compared to APP/PS1 mice (Figure 3 D, E). Aβ plaques were detected in hippocampal and/or cortical region of all groups except WT mice, however, Aβ plaque deposition was significantly reduced in CDHP groups (Figure 3 F, G). These findings imply CDHP exerts neuroprotective effects by reducing Aβ plaque deposition in the brain of APP/PS1 mice.

Fig. 3 CDHP increased dendritic spine density and reduced Aβ plaques in the brain of APP/PS1 Mice. A. Example images of various dendritic spine types. B. Representative images of Golgi staining of dendritic spines across groups. Scale Bar=10 μm. C. Statistical analysis of dendritic spine density per 10 μm dendrites (n=3). D, E. Representative immunoblots and quantitative analyses of SYN and PSD-95 expression in mouse brain tissues (n=3). F. Representative images of the hippocampal region in each group and the area of Aβ plaques in cortical areas. Scale bar=100 or 200 μm. G. Percentage area of Aβ plaques of the brain in mouse brain (n=3). Data are presented as mean ± SEM. $^{###}p< 0.01$ compared with the WT group. $^{***}p<0.01$, $^{**}p<0.01$, $^{*}p<0.05$, compared with the APP/PS1 group.

3.4 CDHP inhibited neuronal apoptosis in vivo and in vitro

Neuronal cell death is a hallmark of neurodegenerative diseases, including PD and AD, with significant neuronal loss observed in key brain regions related to learning and memory (Chi et al., 2018). TUNEL staining was performed to assess neuronal apoptosis in the hippocampal region, and it showed a significantly higher number of apoptotic cells in APP/PS1 mice. The number of positive cells was lower in CDHP groups (Figure 4 A). Additionally, CDHP treatment significantly enhanced the expression of Bcl-2/Bax and decreased the levels of Cleaved Caspase-12 in the brain of APP/PS1 mice (Figure 4 B) and in HT-22 cells (Figure 4 C, D). These results suggest CDHP reduces neuronal apoptosis in APP/PS1 mice and $A\beta_{25-35}$-induced HT22 cells especially in high does group.

Fig. 4 CDHP inhibited neuronal apoptosis in vivo and in vitro. A. Representative images of TUNEL (green)/DAPI (blue) staining in the CA1 and CA3 regions of mouse mice (n=3). Scale bar=100 μm. Quantification of TUNEL-positive cells in each region. B. Representative immunoblots and quantitative analyses of Bcl-2, Bax, Cleaved Caspase-12, and GAPDH of mice brain (n=3). C. Representative immunoblots and quantitative analyses of Bcl-2, Bax, Cleaved Caspase-12, and GAPDH in HT-22 cells (n=3). D. Representative images with quantification of Hoechst 33258 staining in HT-22 cells (n=3). Scale bar=100 μm. Data are presented as mean ± SEM. $^{###}p<0.001$, $^{##}p<0.01$, compared with the WT or Control groups. $^{***}p<0.001$, $^{*}p< 0.05$, compared to the APP/PS1 or $A\beta_{25-35}$ groups.

3.5 CDHP improved mitophagy through mitochondrial morphology and function in AD-like models

Abnormal neuronal apoptosis is often associated with mitochondria dysfunction. Mitochondria are essential for providing energy necessary for neuronal survival. Damaged mitochondria adversely affect neuronal structure and function, leading to energy deficits and the release of harmful substances that promote neuronal apoptosis. TEM images indicated that the morphology of mitochondria in the hippocampus of APP/PS1 mice was different to wild type mice, with blurred membrane boundaries and ridge, as well as damaged mitochondria with content leakage. However, the incidence of abnormal mitochondria significantly decreased following CDHP treatment (Figure 5

A). Additionally, in Aβ$_{25-35}$-induced HT-22 cells, CDHP-H markedly increased the levels of COXIV, a marker of mitochondrial function, (Figure 5 B). Levels of ROS in Aβ$_{25-35}$ treated cells were significantly decreased by CDHP in a dose dependent manner (Figure 5 C, D), suggesting that CDHP improves mitochondrial function in AD-like models.

The clearance of damaged mitochondria is primarily facilitated through mitophagy. TEM revealed that mitophagy-autophagosomes were nearly absent in the hippocampus of APP/PS1 mice compared to WT mice (Figure 6 A). CDHP treatment, prevented the reduction in mitophagy-autophagasomes. The expression levels of mitophagy substrate protein p62 was high and the autophagy marker protein LC3B was low in APP/PS1 mice compared to WT and Aβ$_{25-35}$-induced HT-22 cells compared to control but CDHP treatment restored levels to those seen in the WT animals (Figure 6 B) and non-induced HT-22 cells (Figure 6 C). All of the results shows that the CDHP treatment promote the mitophagy in AD.

Fig. 5 CDHP improved mitochondrial morphology and function in AD-like models. A. TEM results depicting mitochondrial morphology in the hippocampus (n=3). Scale bar =500 nm. B. Representative immunoblots and quantitative analyses of COX IV and GAPDH in Aβ$_{25-35}$-induced HT-22 cells (n=3). C-D. Immunofluorescence was used to detect the levels of ROS in HT-22 cells (n=3). Scale bar =100 μm. Data are presented as mean ± SEM. $^{###}p<0.001$ compared with the Control group. $^{*}p<0.05$, compared with the Aβ$_{25-35}$ group.

Fig. 6 CDHP improved mitophagy in vivo and in vitro. A. Representative TEM images of mitophagy in APP/PS1 mice (n=3). Scale bar=1 μm. B. Representative immunoblots and quantitative analyses of p62, LC3B and β-actin in mice (n=3). C. Representative immunoblots and quantitative analyses of p62, LC3B and β-actin in HT-22 cells. Data are presented as mean ± SEM. $^{###}p<0.001$, $^{##}p<0.01$ compared with the WT or Control groups. $^{***}p<0.001$, $^{**}p<0.01$, $^{*}p<0.05$, compared with the APP/PS1 or Aβ$_{25-35}$ groups.

3.6 CDHP enhanced PGAM5 and FUNDC1 in vivo and in vitro

To uncover the potential for CHDP to stimulate mitophagy, we used molecular docking of CHDP constituents with the mitochondrial phosphatase, Phosphoglycerate mutase family member 5 (PGAM5), a key driver of mitophagy. Eight bioactive constituents of CDHP were identified by TCMSP, the 2D structure data structure of them also list in Table 2, they are sitosterol, myricanone, mandenol, wallichilide,

senkyunone, perlolyrine, FA and stigmasterol. Subsequently, eight active ingredients were molecularly docked with PGAM5. Studies have shown that in molecular docking, when the affinity value is negative, it indicates that the molecule can bind to the protein. The smaller the value, the stronger the binding force between the two (Alsedfy et al., 2024). When the affinity is less than -7, it has a strong binding ability (Cui et al., 2020). Among the eight bioactive ingredients, except for mandenol, the affinity is $\leqslant$-7 (Table 3) (Figure 7 A). The data indicates that the bioactive ingredients of CDHP could exert therapeutic effects by interacting with PGAM5.

To test the relationship between CDHP and PGAM5, the expression level of PGAM5 protein was measured. The brain tissue of APP/PS1 mice and HT-22 cells intervened by $A\beta_{25-35}$ was detected, and it was found that as predicted above, the protein level of PGAM5 in the AD model decreased significantly, and after the administration of CDHP, the expression level of PGAM5 increased significantly (Figure 7 B,C). This result suggests that CDHP may exhibit neuroprotection through increasing PGAM5.

Previous studies have indicated that the levels of mitophagy-related protein FUNDC1 diminished in AD cell models, and promoting FUNDC1-mediated mitophagy can protect neuronal function and mitigate stress-induced damage (Fang et al., 2019). Under normal conditions, the Ser13 and Tyr18 phosphorylation sites of FUNDC1 remain highly phosphorylated, inhibiting its interaction with LC3 and thereby preventing mitophagy. During mitochondrial depolarization and hypoxia, these phosphorylation sites are dephosphorylated, activating FUNDC1 and promoting its binding to LC3, which facilitates mitophagy (Cai et al., 2021; Yang et al., 2024). The FUNDC1 was mediated by Casein Kinase 2, Steroid receptor coactivator, ULK1 or PGAM5 (Liu et al., 2022). The expression level of FUNDC1 was increased significantly with the administration of CDHP (Figure S2).To sum up, we presumed the CDHP improve the expression of PGAM5, which is medicated the FUNDC1 to promote the mitophagy in AD.

Fig. 7 The bioactive ingredients in CDHP play a key role via PGAM5. A. Visualization results of molecular docking between bioactive ingredients in CDHP and PGAM5. B-C. Representative immunoblots and quantitative analyses of PGAM5 and β-actin in APP/PS1 mice brain and HT-22 cells (n=3). Data are presented as mean ± SEM.

$^{###}p<0.001$, compared with the WT or Control group. $^{***}p<0.001$, compared with the APP/PS1 or $A\beta_{25-35}$ group.

4 Discussion

Here we show that CDHP treatment significantly ameliorated cognitive impairment in the APP/PS1 model of AD. CDHP treatment appeared to reverse neuronal atrophy by enhancing the number of dendritic spines and reducing the presence of Aβ plaques in the brain. CDHP treatment was associated with an increase in the expression of mitochondrial proteins and a rise in the number of mitophagy bodies following CDHP administration. Mitophagy is a particular form of autophagy, that clears damaged or dysfunctional mitochondria, thereby contributing to cellular health and viability. This process is particularly vital in high energy-demanding cells, such as neurons, and is associated with various pathologies, including AD and Parkinson's disease. Furthermore, CDHP promoted the expression of PAGM5 and FUNDC1, 2 important proteins involved in mitophagy, suggesting a mechanism by which CDHP may promote mitophagy.

Angelica sinensis (Oliv.) Diels, a traditional Chinese medicinal herb, along with its root and extracts, has been shown to play a vital role in the treatment of various diseases, particularly those affecting the nervous system (Gao et al., 2023; Zeng et al., 2022). Similarly, the *Ligusticum sinense 'Chuanxiong'* exhibits comparable therapeutic properties. Evidence suggests that Ligustilide, the primary active compound derived from *Ligusticum chuanxiong hort* and *Angelica sinensis (Oliv.) Diels*, has neuroprotective effects in models of cerebral ischemia-reperfusion injury (Mao et al., 2022). Additionally, Polysaccharides, extracted different parts of *Angelica sinensis* root, have been reported to alleviate oxidative stress and exhibit anti-inflammatory and anti-oxidative properties in LPS-induced IPEC-J2 cells (Zou et al., 2022). Another study indicated that Angelica sinensis polysaccharide, when combined with Cisplatin, inhibited the expression of the key gene GPX4, promoting the ferroptosis and limiting the migration and invasion of ovarian cancer cells (W. Guo et al., 2024). Furthermore, Ligusticum chuanxiong Hort has been shown to facilitate the proliferation of neural stem cell, neurogenesis, and the preservation of mature neuron (Yu et al., 2021), as well

as to exert anti-neuroinflammation effects and stimulate the production of neural differentiation factor in rats following ischemia injury (Wang et al., 2020). Collectively, these findings support the protective effects of *Angelica sinensis (Oliv.) Diels* and Ligusticum sinense '*Chuanxiong*' across various disease contexts. In this study, we assert that CDHP exhibits neuroprotective activity in APP/PS1 mice and $A\beta_{25-35}$-induced HT-22 cells.

Our results demonstrate that CDHP ameliorates cognitive impairment and inhibits neuronal apoptosis in both APP/PS1 mice and HT-22 cells. Thus, we hypothesize a relationship between CDHP and mitochondrial function, which aligns with previous research findings. Mitophagy is a crucial mechanism for the removal of dysfunctional mitochondria and the maintenance of mitochondrial function, thereby ensuring intracellular homeostasis (Picca et al., 2023; Wang et al., 2023). Impaired mitophagy may exacerbate Aβ and tau pathologies through mechanisms involving oxidative stress, microglial activation, and chronic inflammation in AD (Song et al., 2021). Recent study has shown that long-term treatment with Urolithin A significantly enhances learning and memory functions in APP/PS1 mice by inducing mitophagy through the enhancement of cellular lysosomal functions (Hou et al., 2024). Similar findings have been reported for melatonin, which restored mitophagy by improving mitophagosome-lysosome fusion, reducing Aβ pathology, and enhancing cognition in transgenic mice (Chen et al., 2021). In our work, we posited a connection between CDHP and mitochondrial function. Subsequent transmission electron microscopy and Western Blot analyses revealed reduction in the number of abnormal mitochondria and elevation in the expression of mitochondrial function proteins following CDHP treatment in APP/PS1 mice and $A\beta_{25-35}$ induced HT-22 cells models. Interestingly, the number of mitophagy bodies increased in the hippocampus of APP/PS1 mice, while the levels of mitophagy substrate protein p62 decreased, and autophagy marker protein LC3B increased following CDHP treatment. Thus, we assert that CDHP enhances mitophagy in AD, and our data corroborate the notion that restored or improved mitophagy is beneficial for cognitive enhancement in this context. Unlike other pharmacological

agents or mechanisms, we propose that CDHP exerts its neuroprotective effects through mitophagy in AD. Traditional Chinese medicine has the characteristic of multi-target pharmacological effects. Therefore, our findings provide experimental evidence that CDHP treatment may alleviate cognitive dysfunction by improving mitophagy in AD.

Dendritic spines serve as the primary sites for synapse formation between neurons, their alterations are indicative of synaptic plasticity, which is essential for learning and long-term memory processes (Barrantes, 2024). Recent studies have demonstrated that in psychiatric patients elevated expression of NISCH lead to changed dendritic spine morphogenesis and impaired working memory (Yang et al., 2023). Additionally, early tau-related deficits have been linked to the accumulation of hyperphosphorylated tau within normal dendritic spines (Hoover et al., 2010). In our study, we observed a decrease in the number of functional dendritic spines in APP/PS1 mice, accompanied by an increase in Aβ plaques in the brain. Notably, the average percentage of stubby and mushroom-like dendritic spines in mice with CDHP was higher than that in APP/PS1 mice, and the levels of SYN and PSD-95 also increased in CDHP groups.

Mitophagy primarily involves two pathways, PINK1/Parkin-mediated pathway and the receptor-mediated pathway(Li et al., 2023). While PINK1/Parkin-mediated mitophagy pathway has been shown to play significant roles in neurodegenerative diseases in both murine models and Drosophila melanogaster with Parkin/PINK1 deficiencies, the body can compensate through a receptor-mediated mitophagy pathway that primarily involves mitochondrial membrane receptor proteins, such as FUNDC1, BNIP3 and NIX (D'Arcy, 2024). Shen-fu Injection activates the HIF- 1α/BNIP3 pathway to mediate mitophagy in ischemia-reperfusion injury(Chen et al., 2025), BNIP3-mediated mitophagy regulates the glycolytic shift and pro-inflammatory polarization in macrophages in obesity-related metabolic diseases(Kim et al., 2025), as well as NIX mediated mitophagy(X. Zhou et al., 2024). Thus, the receptor-mediated pathway is plays an essential role in diverse disease. FUNDC1 has been shown to preserve chondrocyte homeostasis by triggering mitophagy, with FUNDC1 knockdown or knockout leading to decreased mitophagy and exacerbated mitochondrial

dysfunction in osteoarthritis progression (Fang et al., 2023). Actived PGAM5 dephosphorylates FUNDC1 to initiate mitophagy. The reciprocal interaction of PGAM5 with FUNDC1 and BCL-xL, mediated by PGAM5 multimerization, work on mitophagy and apoptosis (Ma et al., 2020). Our dada shown that the CDHP treatment promoted mitophagy, and enhanced the expression of PGAM5 and FUNDC1.

5 Conclusion

In summary, CDHP has been shown to improve cognitive deficits and exert neuroprotective effects in APP/PS1 mice and $A\beta_{25-35}$-induced HT-22 cells. These effects correlate with a stimulated increase in mitophagy in vivo, and increased expression of PGAM5/FUNDC1. Our data highlight a potential mechanism for the neuroprotective effect of CDHP in AD and uncover a potential avenue for future therapeutic approaches.

Credit author statement

Keting Pu: Investigation, Methodology, Formal analysis, Validation, Visualization, Writing – original draft. **Simin Yang:** Investigation, Methodology, Validation. **Ruilin Sheng:** Methodology, Validation, Investigation. **Jie Chen:** Investigation. **Yuan Dai:** Supervision. **Ian C Wood:** Conceptualization, Supervision, revise & editing**. Zhanqiong Zhong:** Conceptualization, Funding acquisition, Investigation, Supervision, Methodology, Writing – original draft, Writing – review & editing. **Shijun Xu:** Design, Conceptualization, Data curation, Supervision, Writing – revise & editing, Funding acquisition. The authors agree to be responsible for all aspects of the manuscript ensuring the accuracy and integrity.

Declaration of competing interest

The authors declare that they have no known competing financial interests or personal relationships that could have appeared to influence the work reported in this paper.

Funding

This work was supported by National Natural Science Foundation of China (No. 82274240; No. 82074150,); Xinglin Scholars Project of Chengdu University of TCM (XJ2023001201; SYJS2024001).

Data availability

Data will be made available on request

Supplements

Fig. S1 A. Non-toxic concentration of CDHP on HT-22 cells (n=6). B. Concentrations of $A\beta_{25-35}$ intervention in the HT-22 cell model (n=6). C. Effects of different concentrations of CDHP on HT-22 cells with $A\beta_{25-35}$ intervention (n=6). Data are presented as mean ± SEM. $^{###}p<0.001$, $^{##}p<0.01$, $^{#}p<0.05$ compared with the Control group. $^{***}p<0.001$ compared with the $A\beta_{25-35}$ group.

Fig. S2 Representative immunoblots and quantitative analyses of FUNDC1, PGAM5 and β-actin (n=3). Data are presented as mean ± SEM. $^{###}p<0.001$ compared with the WT or Control groups. $^{**}p<0.01$, $^{*}p<0.05$, compared with the APP/PS1 or $A\beta_{25-35}$ groups.

Alsedfy, M.Y., Ebnalwaled, A.A., Moustafa, M., Said, A.H., 2024. Investigating the binding affinity, molecular dynamics, and ADMET properties of curcumin-IONPs as a mucoadhesive bioavailable oral treatment for iron deficiency anemia. Sci Rep 14, 22027. https://doi.org/10.1038/s41598-024-72577-8

Barrantes, F.J., 2024. Cognitive synaptopathy: synaptic and dendritic spine dysfunction in age-related cognitive disorders. Front Aging Neurosci 16, 1476909. https://doi.org/10.3389/fnagi.2024.1476909

Cai, Y., Yang, E., Yao, X., Zhang, X., Wang, Q., Wang, Y., Liu, J., Fan, W., Yi, K., Kang, C., Wu, J., 2021. FUNDC1-dependent mitophagy induced by tPA protects neurons against cerebral ischemia-reperfusion injury. Redox Biol 38, 101792. https://doi.org/10.1016/j.redox.2020.101792

Cao, J., Tang, Y., Li, Y., Gao, K., Shi, X., Li, Z., 2017. Behavioral Changes and Hippocampus Glucose Metabolism in APP/PS1 Transgenic Mice via Electro-acupuncture at Governor Vessel Acupoints. Front Aging Neurosci 9, 5. https://doi.org/10.3389/fnagi.2017.00005

Chen, C., Yang, C., Wang, J., Huang, X., Yu, H., Li, Shangming, Li, Shupeng, Zhang, Z., Liu, J., Yang, X., Liu, G.-P., 2021. Melatonin ameliorates cognitive deficits through improving mitophagy in a mouse model of Alzheimer's disease. J Pineal Res 71, e12774. https://doi.org/10.1111/jpi.12774

Chen, M., Chen, Z., Wang, Y., Tan, Z., Zhu, C., Li, Y., Han, Z., Chen, L., Gao, R., Liu, L., Chen, Q., 2016. Mitophagy receptor FUNDC1 regulates mitochondrial dynamics and mitophagy. Autophagy 12, 689–702. https://doi.org/10.1080/15548627.2016.1151580

Chen, Y., Peng, F., Yang, C., Hou, H., Xing, Z., Chen, J., Liu, L., Peng, C., Li, D., 2023. SIRT1 activation by 2,3,5,6-tetramethylpyrazine alleviates neuroinflammation via inhibiting M1 microglia polarization. Front Immunol 14, 1206513. https://doi.org/10.3389/fimmu.2023.1206513

Chen, Y., Wei, J., Zhang, Y., Sun, W., Li, Z., Wang, Q., Xu, X., Li, C., Li, P., 2018. Anti-endometriosis Mechanism of Jiawei Foshou San Based on Network Pharmacology. Front Pharmacol 9, 811. https://doi.org/10.3389/fphar.2018.00811

Chen, Z., Liu, T., Xiong, L., Liu, Z., 2025. Shen-fu Injection Modulates HIF- 1α/BNIP3-Mediated Mitophagy to Alleviate Myocardial Ischemia–Reperfusion Injury. Cardiovasc Toxicol. https://doi.org/10.1007/s12012-025-09993-3

Chi, H., Chang, H.-Y., Sang, T.-K., 2018. Neuronal Cell Death Mechanisms in Major Neurodegenerative Diseases. Int J Mol Sci 19, 3082. https://doi.org/10.3390/ijms19103082

Costa-Mattioli, M., Gobert, D., Harding, H., Herdy, B., Azzi, M., Bruno, M., Bidinosti, M., Mamou, C.B., Marcinkiewicz, E., Yoshida, M., Imataka, H., Claudio Cuello, A., Seidah, N., Sossin, W., Lacaille, J.-C., Ron, D., Nader, K., Sonenberg, N., 2005. Translational control of hippocampal synaptic plasticity and memory by the eIF2α kinase, GCN2. Nature 436, 1166–1173. https://doi.org/10.1038/nature03897

Cui, Q., Zhang, Y., Ma, Y., Yu, H., Zhao, X., Zhang, L., Ge, S., Zhang, G., Qin, X., 2020. A network pharmacology approach to investigate the mechanism of Shuxuening injection in the treatment of ischemic stroke. Journal of Ethnopharmacology 257, 112891. https://doi.org/10.1016/j.jep.2020.112891

D'Arcy, M.S., 2024. Mitophagy in health and disease. Molecular mechanisms, regulatory pathways, and therapeutic implications. Apoptosis. https://doi.org/10.1007/s10495-024-01977-y

Du, Q., Zhu, X., Si, J., 2020. Angelica polysaccharide ameliorates memory impairment in Alzheimer's disease rat through activating BDNF/TrkB/CREB pathway. Exp Biol Med (Maywood) 245, 1–10. https://doi.org/10.1177/1535370219894558

Fairley, L.H., Grimm, A., Herff, S.A., Eckert, A., 2024. Translocator protein (TSPO) ligands attenuate mitophagy deficits in the SH-SY5Y cellular model of Alzheimer's disease via the autophagy adaptor P62. Biochimie 224, 132–138. https://doi.org/10.1016/j.biochi.2024.01.012

Fang, E.F., Hou, Y., Palikaras, K., Adriaanse, B.A., Kerr, J.S., Yang, B., Lautrup, S., Hasan-Olive, M.M., Caponio, D., Dan, X., Rocktäschel, P., Croteau, D.L., Akbari, M., Greig, N.H., Fladby, T., Nilsen, H., Cader, M.Z., Mattson, M.P., Tavernarakis, N., Bohr, V.A., 2019. Mitophagy inhibits amyloid-β and tau pathology and reverses cognitive deficits in models of Alzheimer's disease. Nat Neurosci 22, 401–412. https://doi.org/10.1038/s41593-018-0332-9

Fang, G., Wen, X., Jiang, Z., Du, X., Liu, R., Zhang, C., Huang, G., Liao, W., Zhang, Z., 2023. FUNDC1/PFKP-mediated mitophagy induced by KD025 ameliorates cartilage degeneration in osteoarthritis. Mol Ther 31, 3594–3612. https://doi.org/10.1016/j.ymthe.2023.10.016

Gao, Y., Mo, S., Cao, H., Zhi, Y., Ma, X., Huang, Z., Li, B., Wu, J., Zhang, K., Jin, L., 2023. The efficacy and mechanism of Angelica sinensis (Oliv.) Diels root aqueous extract based on RNA sequencing and 16S rDNA sequencing in alleviating polycystic ovary syndrome. Phytomedicine 120, 155013. https://doi.org/10.1016/j.phymed.2023.155013

Gao, Y., Yang, Z., Ji, T., Zhou, P., Geng, L., Gao, X., 2024. Anti-papillary thyroid carcinoma effects of *dioscorea bulbifera* L. through ferroptosis and the PI3K/AKT pathway based on network pharmacology and experimental validation. Journal of Ethnopharmacology 326, 117912. https://doi.org/10.1016/j.jep.2024.117912

Günther, M., Dabare, S., Fuchs, J., Gunesch, S., Hofmann, J., Decker, M., Culmsee, C., 2023. Flavonoid-Phenolic Acid Hybrids Are Potent Inhibitors of Ferroptosis via Attenuation of Mitochondrial Impairment. Antioxidants (Basel) 13, 44. https://doi.org/10.3390/antiox13010044

Guo, W., Wang, W., Lei, F., Zheng, R., Zhao, X., Gu, Y., Yang, M., Tong, Y., Wang, Y., 2024. Angelica sinensis polysaccharide combined with cisplatin reverses cisplatin resistance of ovarian cancer by inducing ferroptosis via regulating GPX4. Biomed Pharmacother 175, 116680. https://doi.org/10.1016/j.biopha.2024.116680

Guo, X., Zhang, Z., Gu, J., Ke, P., Liu, J., Meng, Y., Zheng, W., Que, W., Fan, R., Luo, J., Xiao, F., 2024. FUDNC1-dependent mitophagy ameliorate motor neuron death in an amyotrophic lateral sclerosis mouse model. Neurobiol Dis 197, 106534. https://doi.org/10.1016/j.nbd.2024.106534

Hoover, B.R., Reed, M.N., Su, J., Penrod, R.D., Kotilinek, L.A., Grant, M.K., Pitstick, R., Carlson, G.A., Lanier, L.M., Yuan, L.-L., Ashe, K.H., Liao, D., 2010. Tau mislocalization to dendritic spines mediates synaptic dysfunction independently of neurodegeneration. Neuron 68, 1067–1081. https://doi.org/10.1016/j.neuron.2010.11.030

Hou, Y., Chu, X., Park, J.-H., Zhu, Q., Hussain, M., Li, Z., Madsen, H.B., Yang, B., Wei, Y., Wang, Y., Fang, E.F., Croteau, D.L., Bohr, V.A., 2024. Urolithin A improves Alzheimer's disease cognition and restores mitophagy and lysosomal functions. Alzheimers Dement 20, 4212–4233. https://doi.org/10.1002/alz.13847

Kasai, H., Ucar, H., Morimoto, Y., Eto, F., Okazaki, H., 2023. Mechanical transmission at spine synapses: Short-term potentiation and working memory. Curr Opin Neurobiol 80, 102706.

https://doi.org/10.1016/j.conb.2023.102706

Katayama, H., Hama, H., Nagasawa, K., Kurokawa, H., Sugiyama, M., Ando, R., Funata, M., Yoshida, N., Homma, M., Nishimura, T., Takahashi, M., Ishida, Y., Hioki, H., Tsujihata, Y., Miyawaki, A., 2020. Visualizing and Modulating Mitophagy for Therapeutic Studies of Neurodegeneration. Cell 181, 1176-1187.e16. https://doi.org/10.1016/j.cell.2020.04.025

Kim, S., Choi ,Cheoljun, Son ,Yeonho, Lee ,Junhyuck, Joo ,Sungug, and Lee, Y.-H., 2025. BNIP3-mediated mitophagy in macrophages regulates obesity-induced adipose tissue metaflammation. Autophagy 0, 1–19. https://doi.org/10.1080/15548627.2025.2487035

Lee, J.J., Sanchez-Martinez, A., Martinez Zarate, A., Benincá, C., Mayor, U., Clague, M.J., Whitworth, A.J., 2018. Basal mitophagy is widespread in Drosophila but minimally affected by loss of Pink1 or parkin. J Cell Biol 217, 1613–1622. https://doi.org/10.1083/jcb.201801044

Li, G., Li, J., Shao, R., Zhao, J., Chen, M., 2021. FUNDC1: A Promising Mitophagy Regulator at the Mitochondria-Associated Membrane for Cardiovascular Diseases. Front Cell Dev Biol 9, 788634. https://doi.org/10.3389/fcell.2021.788634

Li, J., Yang, D., Li, Z., Zhao, M., Wang, D., Sun, Z., Wen, P., Dai, Y., Gou, F., Ji, Y., Zhao, D., Yang, L., 2023. PINK1/Parkin-mediated mitophagy in neurodegenerative diseases. Ageing Research Reviews 84, 101817. https://doi.org/10.1016/j.arr.2022.101817

Li, K., Xia, X., Tong, Y., 2024. Multiple roles of mitochondrial autophagy receptor FUNDC1 in mitochondrial events and kidney disease. Front Cell Dev Biol 12, 1453365. https://doi.org/10.3389/fcell.2024.1453365

Li, X., Guan, L., Liu, Z., Du, Z., Yuan, Q., Zhou, F., Yang, X., Lv, M., Lv, L., 2024. Ubiquitination of ATAD3A by TRIM25 exacerbates cerebral ischemia-reperfusion injury via regulating PINK1/Parkin signaling pathway-mediated mitophagy. Free Radic Biol Med 224, 757–769. https://doi.org/10.1016/j.freeradbiomed.2024.09.029

Liu, H., Zang, C., Yuan, F., Ju, C., Shang, M., Ning, J., Yang, Y., Ma, J., Li, G., Bao, X., Zhang, D., 2022. The role of FUNDC1 in mitophagy, mitochondrial dynamics and human diseases. Biochemical Pharmacology 197, 114891. https://doi.org/10.1016/j.bcp.2021.114891

Liu, M., Chen, F., Sha, L., Wang, S., Tao, L., Yao, L., He, M., Yao, Z., Liu, H., Zhu, Z., Zhang, Z., Zheng, Z., Sha, X., Wei, M., 2014. (−)-Epigallocatechin-3-Gallate Ameliorates Learning and Memory Deficits by Adjusting the Balance of TrkA/p75NTR Signaling in APP/PS1 Transgenic Mice. Mol Neurobiol 49, 1350–1363. https://doi.org/10.1007/s12035-013-8608-2

Ma, K., Zhang, Z., Chang, R., Cheng, H., Mu, C., Zhao, T., Chen, L., Zhang, C., Luo, Q., Lin, J., Zhu, Y., Chen, Q., 2020. Dynamic PGAM5 multimers dephosphorylate BCL-xL or FUNDC1 to regulate mitochondrial and cellular fate. Cell Death Differ 27, 1036–1051. https://doi.org/10.1038/s41418-019-0396-4

Mao, Z., Tian, L., Liu, J., Wu, Q., Wang, N., Wang, G., Wang, Y., Seto, S., 2022. Ligustilide ameliorates hippocampal neuronal injury after cerebral ischemia reperfusion through activating PINK1/Parkin-dependent mitophagy. Phytomedicine 101, 154111. https://doi.org/10.1016/j.phymed.2022.154111

Mary, A., Eysert, F., Checler, F., Chami, M., 2022. Mitophagy in Alzheimer's disease: Molecular defects and therapeutic approaches. Molecular Psychiatry 28, 202. https://doi.org/10.1038/s41380-022-01631-6

N, W., J, Y., R, C., Y, L., S, L., Y, P., Q, L., Y, W., L, H., Y, S., Z, L., 2023. Ginsenoside Rg1 ameliorates Alzheimer's disease pathology via restoring mitophagy. Journal of ginseng research 47.

https://doi.org/10.1016/j.jgr.2022.12.001

Picca, A., Faitg, J., Auwerx, J., Ferrucci, L., D'Amico, D., 2023. Mitophagy in human health, ageing and disease. Nat Metab 5, 2047–2061. https://doi.org/10.1038/s42255-023-00930-8

Poole, L.P., Macleod, K.F., 2021. Mitophagy in tumorigenesis and metastasis. Cell Mol Life Sci 78, 3817–3851. https://doi.org/10.1007/s00018-021-03774-1

Schmid, E.T., Pyo, J.-H., Walker, D.W., 2022. Neuronal induction of BNIP3-mediated mitophagy slows systemic aging in Drosophila. Nat Aging 2, 494–507. https://doi.org/10.1038/s43587-022-00214-y

She, L., Sun, J., Xiong, L., Li, A., Li, L., Wu, H., Ren, J., Wang, W., Liang, G., Zhao, X., 2024. Ginsenoside RK1 improves cognitive impairments and pathological changes in Alzheimer's disease via stimulation of the AMPK/Nrf2 signaling pathway. Phytomedicine 122, 155168. https://doi.org/10.1016/j.phymed.2023.155168

Skaper, S.D., Facci, L., Zusso, M., Giusti, P., 2017. Synaptic Plasticity, Dementia and Alzheimer Disease. CNS Neurol Disord Drug Targets 16, 220–233. https://doi.org/10.2174/1871527316666170113120853

Song, M., Zhao, X., Song, F., 2021. Aging-Dependent Mitophagy Dysfunction in Alzheimer's Disease. Mol Neurobiol 58, 2362–2378. https://doi.org/10.1007/s12035-020-02248-y

Tian, W., Zhu, M., Zhou, Y., Mao, C., Zou, R., Cui, Y., Li, S., Zhu, J., Hu, C., 2022. Electroacupuncture Pretreatment Alleviates Cerebral Ischemia-Reperfusion Injury by Regulating Mitophagy via mTOR-ULK1/FUNDC1 Axis in Rats. J Stroke Cerebrovasc Dis 31, 106202. https://doi.org/10.1016/j.jstrokecerebrovasdis.2021.106202

Um, J.-H., Shin, D.J., Choi, S.M., Nathan, A.B.P., Kim, Y.Y., Lee, D.Y., Jeong, D.J., Kim, D.H., Kim, K.H., Kim, Y.H., Nah, J., Jeong, J.-H., Yoo, E., Shin, H.K., Park, H.T., Jo, J., Cho, J.H., Yun, J., 2024. Selective induction of Rab9-dependent alternative mitophagy using a synthetic derivative of isoquinoline alleviates mitochondrial dysfunction and cognitive deficits in Alzheimer's disease models. Theranostics 14, 56–74. https://doi.org/10.7150/thno.88718

Wang, M., Yao, M., Liu, J., Takagi, N., Yang, B., Zhang, M., Xu, L., Ren, J., Fan, X., Tian, F., 2020. Ligusticum chuanxiong exerts neuroprotection by promoting adult neurogenesis and inhibiting inflammation in the hippocampus of ME cerebral ischemia rats. J Ethnopharmacol 249, 112385. https://doi.org/10.1016/j.jep.2019.112385

Wang, S., Long, H., Hou, L., Feng, B., Ma, Z., Wu, Y., Zeng, Y., Cai, J., Zhang, D.-W., Zhao, G., 2023. The mitophagy pathway and its implications in human diseases. Signal Transduct Target Ther 8, 304. https://doi.org/10.1038/s41392-023-01503-7

Wei, X., Xiong, X., Wang, P., Zhang, S., Peng, D., 2024. SIRT1-mediated deacetylation of FOXO3 enhances mitophagy and drives hormone resistance in endometrial cancer. Mol Med 30, 147. https://doi.org/10.1186/s10020-024-00915-7

Y, C., E, Y., X, Y., X, Z., Q, W., Y, W., J, L., W, F., K, Y., C, K., J, W., 2021. FUNDC1-dependent mitophagy induced by tPA protects neurons against cerebral ischemia-reperfusion injury. Redox biology 38. https://doi.org/10.1016/j.redox.2020.101792

Yang, K., Yan, Y., Yu, A., Zhang, R., Zhang, Y., Qiu, Z., Li, Z., Zhang, Q., Wu, S., Li, F., 2024. Mitophagy in neurodegenerative disease pathogenesis. Neural Regen Res 19, 998–1005. https://doi.org/10.4103/1673-5374.385281

Yang, Z.-H., Cai, X., Ding, Z.-L., Li, W., Zhang, C.-Y., Huo, J.-H., Zhang, Y., Wang, L., Zhang, L.-M., Li, S.-W., Li, M., Zhang, C., Chang, H., Xiao, X., 2023. Identification of a psychiatric risk gene

NISCH at 3p21.1 GWAS locus mediating dendritic spine morphogenesis and cognitive function. BMC Med 21, 254. https://doi.org/10.1186/s12916-023-02931-6

Yi, J., Wang, H.-L., Lu, G., Zhang, H., Wang, Lina, Li, Z.-Y., Wang, Liming, Wu, Y., Xia, D., Fang, E.F., Shen, H.-M., 2024. Spautin-1 promotes PINK1-PRKN-dependent mitophagy and improves associative learning capability in an alzheimer disease animal model. Autophagy 1–22. https://doi.org/10.1080/15548627.2024.2383145

Yu, B., Yao, Y., Zhang, X., Ruan, M., Zhang, Z., Xu, L., Liang, T., Lu, J., 2021. Synergic Neuroprotection Between Ligusticum Chuanxiong Hort and Borneol Against Ischemic Stroke by Neurogenesis via Modulating Reactive Astrogliosis and Maintaining the Blood-Brain Barrier. Front Pharmacol 12, 666790. https://doi.org/10.3389/fphar.2021.666790

Zeng, P., Su, H.-F., Ye, C.-Y., Qiu, S.-W., Shi, A., Wang, J.-Z., Zhou, X.-W., Tian, Q., 2022. A Tau Pathogenesis-Based Network Pharmacology Approach for Exploring the Protections of Chuanxiong Rhizoma in Alzheimer's Disease. Front Pharmacol 13, 877806. https://doi.org/10.3389/fphar.2022.877806

Zhou, X., Lu, Q., Wang, Q., Chu, W., Huang, J., Yu, J., Nong, Y., Lu, W., 2024. Diltiazem Hydrochloride Protects Against Myocardial Ischemia/Reperfusion Injury in a BNIP3L/NIX-Mediated Mitophagy Manner. J Inflamm Res 17, 8905–8919. https://doi.org/10.2147/JIR.S493037

Zhou, Y., Guo, X., Chen, W., Liu, J., 2019. Angelica polysaccharide mitigates lipopolysaccharide-evoked inflammatory injury by regulating microRNA-10a in neuronal cell line HT22. Artif Cells Nanomed Biotechnol 47, 3194–3201. https://doi.org/10.1080/21691401.2019.1614595

Zhou, Y., Zhao, Q., Zhang, Y., Di, L., Xue, F., Xu, W., Gao, W., Guo, Y., He, Y., Kou, J., Qin, Y., Xie, X., Du, L., Han, G., Pang, X., 2024. A new andrographolide derivative ADA targeting SIRT3-FOXO3a signaling mitigates cognitive impairment by activating mitophagy and inhibiting neuroinflammation in Apoe4 mice. Phytomedicine 124, 155298. https://doi.org/10.1016/j.phymed.2023.155298

Zou, Y.-F., Li, C.-Y., Fu, Y.-P., Jiang, Q.-X., Peng, X., Li, L.-X., Song, X., Zhao, X.-H., Li, Y.-P., Chen, X.-F., Feng, B., Huang, C., Jia, R.-Y., Ye, G., Tang, H.-Q., Yin, Z.-Q., 2022. The comparison of preliminary structure and intestinal anti-inflammatory and anti-oxidative activities of polysaccharides from different root parts of Angelica sinensis (Oliv.) Diels. J Ethnopharmacol 295, 115446. https://doi.org/10.1016/j.jep.2022.115446

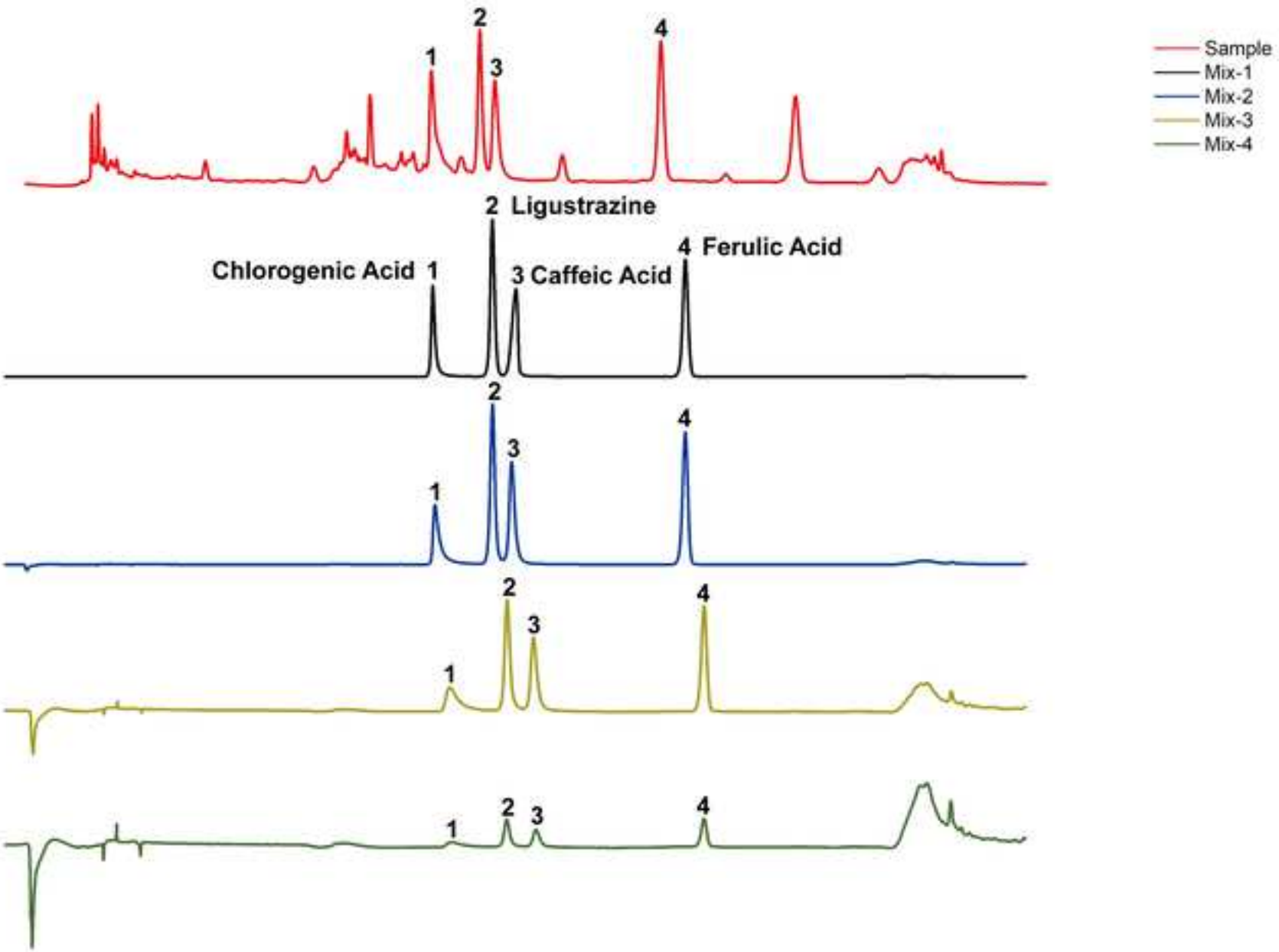

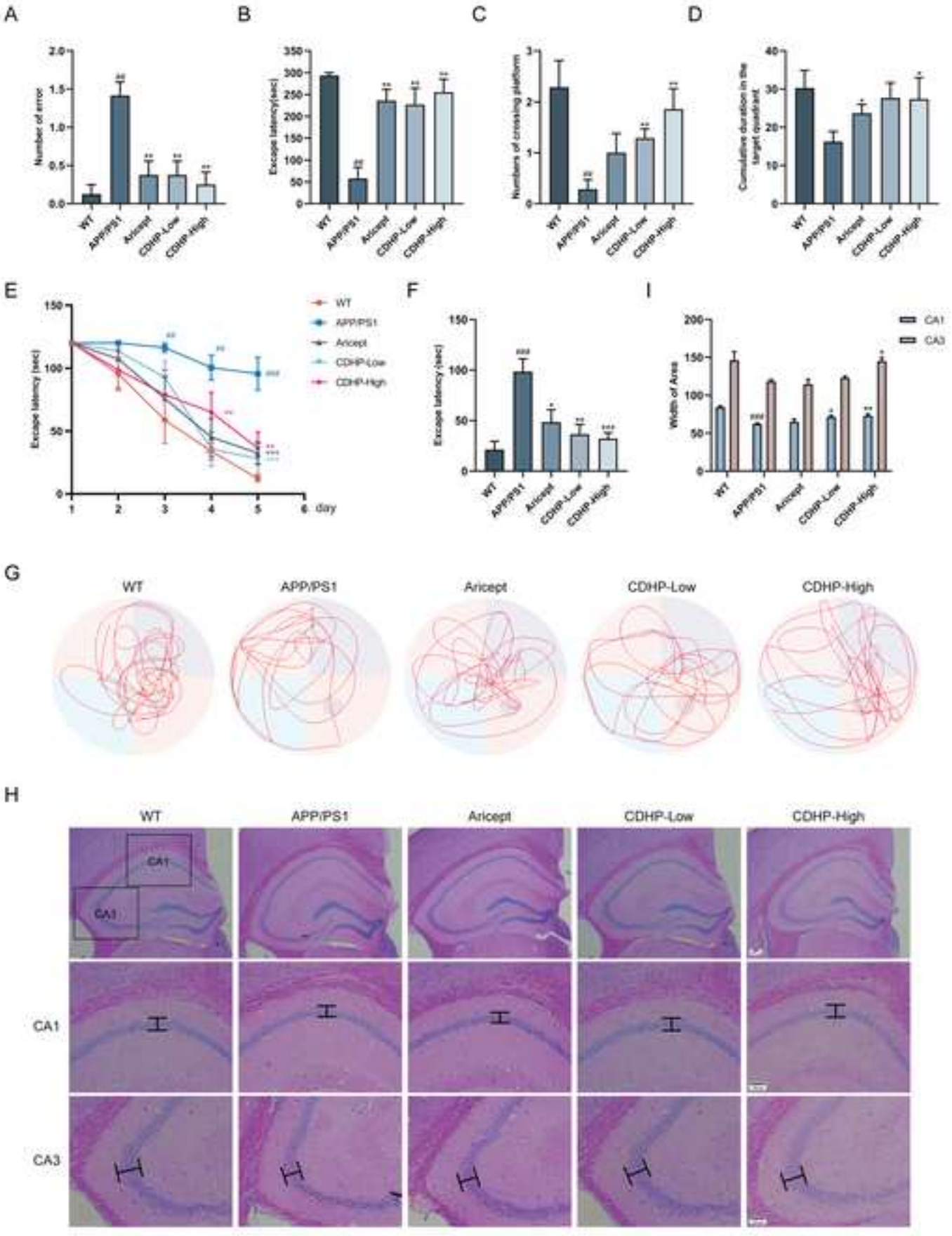

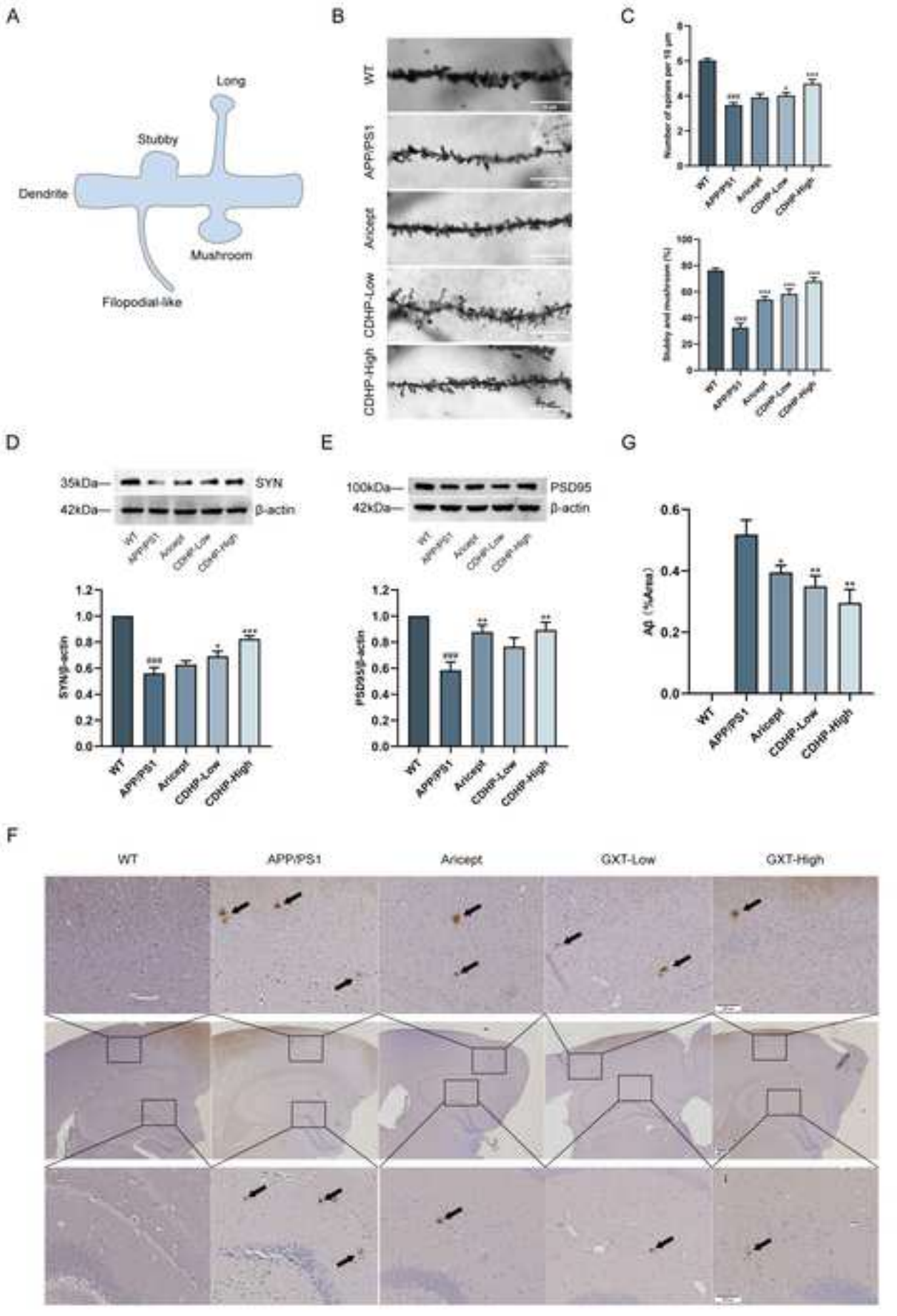

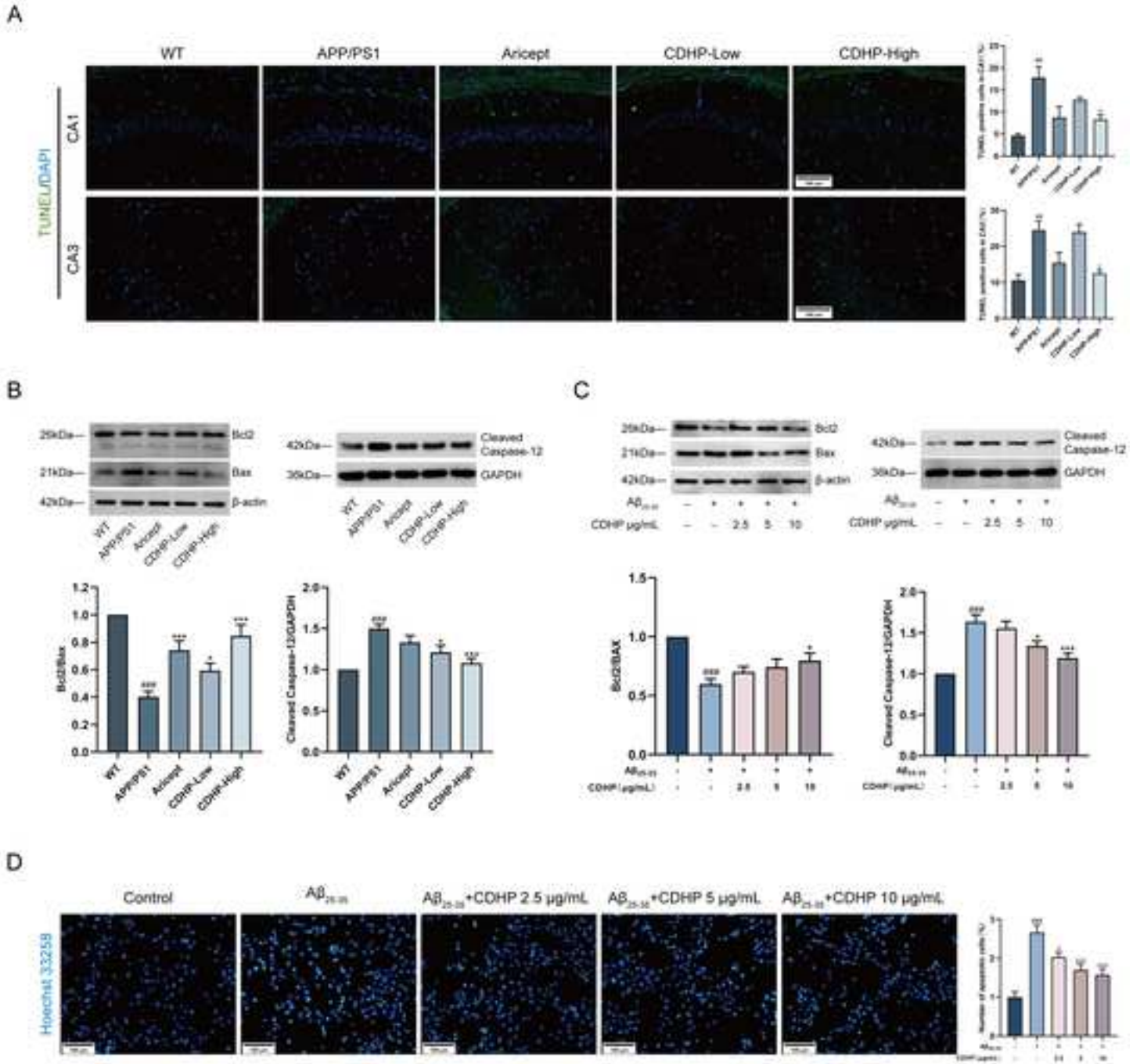

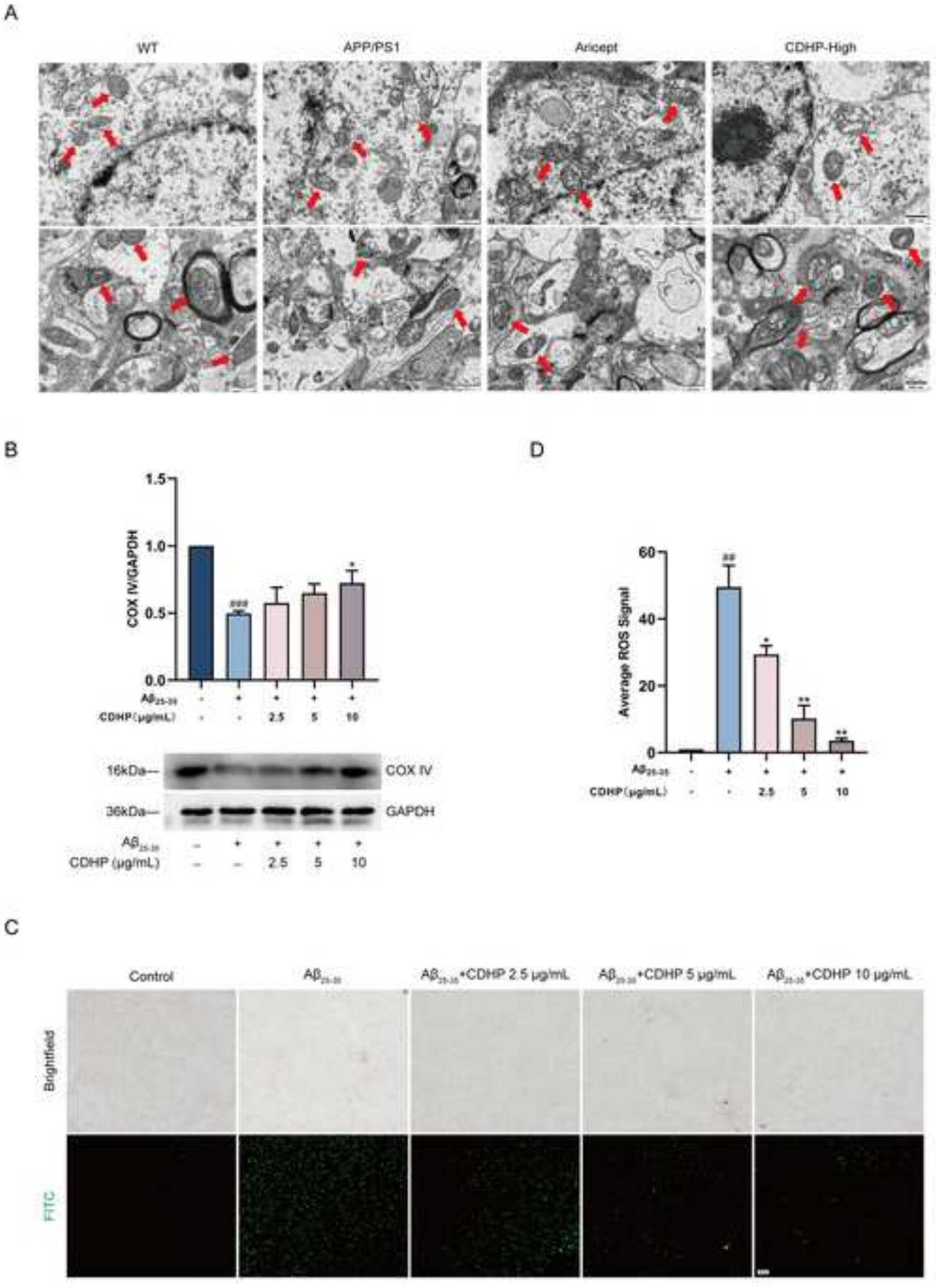

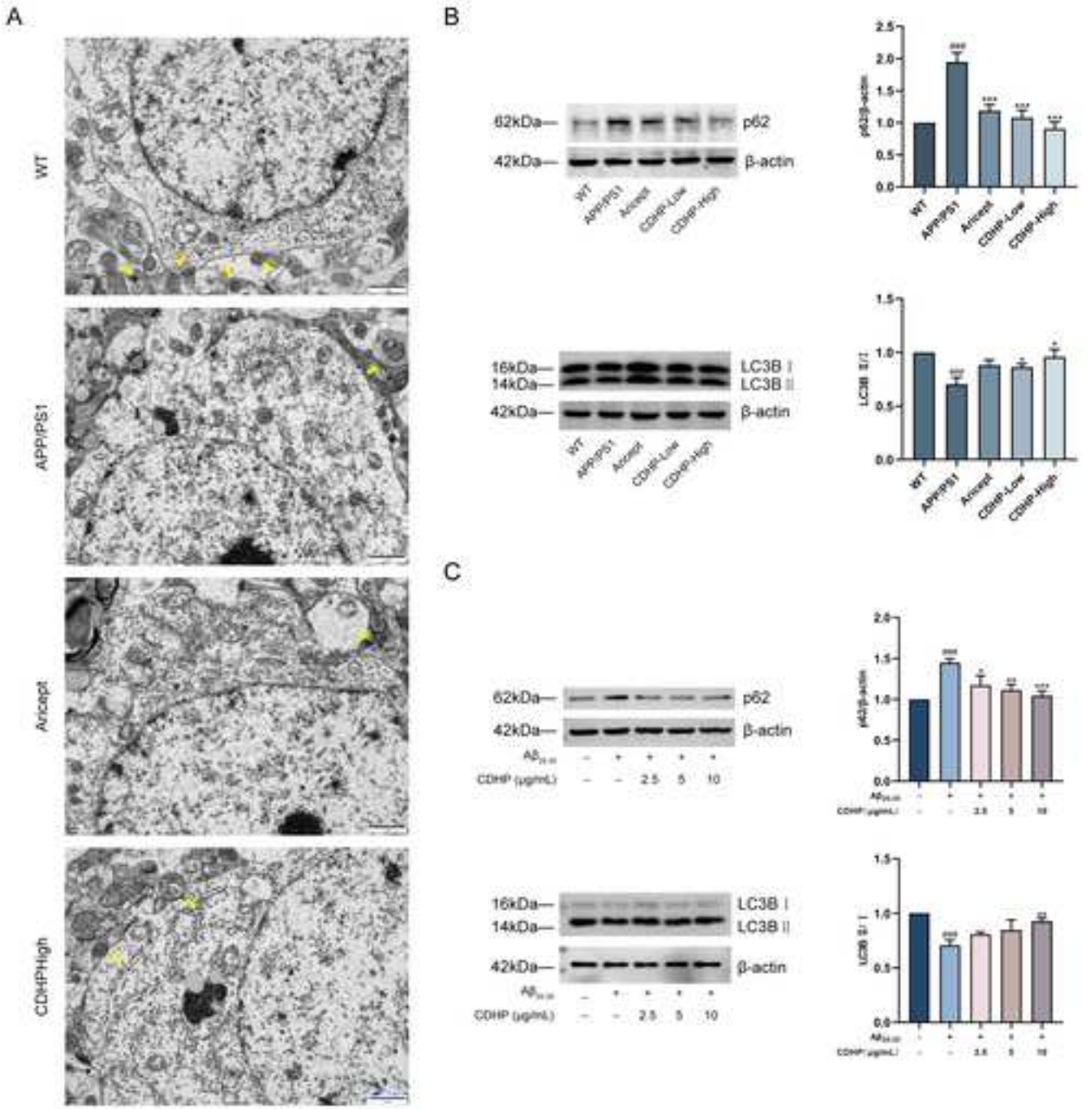

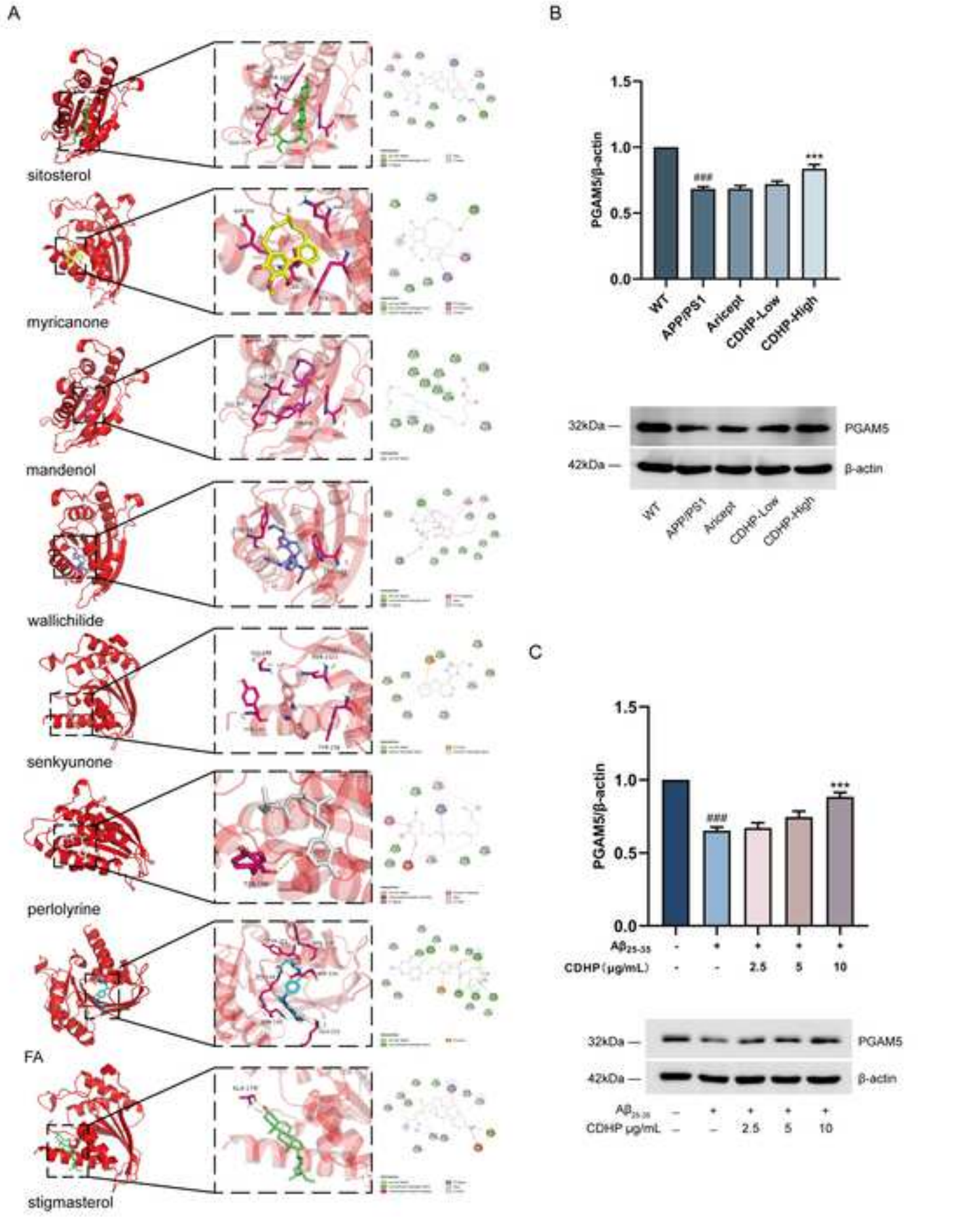

Table 1 Soluble Quantity of the Corresponding Standard in CDHP

	Chemical Compound			
	Chlorogenic Acid	Ligustrazine	Caffeic Acid	Ferulic Acid
Soluble Quantity (mg/g)	0.8744	0.6845	0.3772	0.5824

Table 2 The Bioactive Compounds of CDHP

Mol ID	Molecule Name	2D Structure	WM	OB (%)	DL
MOL000359	sitosterol	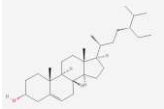	414.79	36.91	0.75
MOL002135	myricanone		356.45	40.60	0.51
MOL001494	mandenol	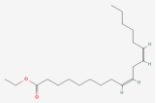	308.56	42.00	0.19
MOL002157	wallichilide	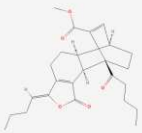	412.57	42.31	0.71
MOL002151	senkyunone	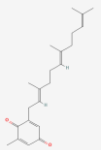	326.52	47.66	0.24
MOL002140	perlolyrine		264.30	65.95	0.27
MOL000433	FA	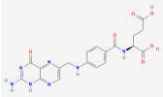	441.45	68.96	0.71
MOL000449	stigmasterol		412.77	43.83	0.76

Table 3 The Affinities of Bioactive Constituents of CDHP with PGAM5

Molecule Name	Affinity (kcal/mol)	rmsd l.b.	rmsd u.b.
sitosterol	-8.1	0.000	0.000
myricanone	-7.5	0.000	0.000
mandenol	-5.3	0.000	0.000
wallichilide	-7.4	0.000	0.000
senkyunone	-7.4	0.000	0.000
perlolyrine	-7.0	0.000	0.000
FA	-8.2	0.000	0.000
stigmasterol	-8.2	0.000	0.000

Declaration of Interest Statement

The authors declare that they have no known competing financial interests or personal relationships that could have appeared to influence the work reported in this article.

Keting Pu, Simin Yang, Ruilin Sheng, Jie Chen, Yuan Dai, Ian C Wood, Zhanqiong Zhong, Shijun Xu